IIE Transactions

ISSN: 0740-817X (Print) 1545-8830 (Online) Journal homepage: http://www.tandfonline.com/loi/uiie20

Fairing the gamma: an engineering approach to sensitivity estimation

Wanmo Kang , Kyoung-Kuk Kim & Hayong Shin

To cite this article: Wanmo Kang , Kyoung-Kuk Kim & Hayong Shin (2014) Fairing the gamma: an engineering approach to sensitivity estimation, IIE Transactions, 46:4, 374-396, DOI: 10.1080/0740817X.2012.689125

To link to this article: http://dx.doi.org/10.1080/0740817X.2012.689125

Accepted author version posted online: 10 Jul 2012.
Published online: 10 Jul 2012.

IIE Transactions (2014) **46**, 374–396

ISSN: 0740-817X print / 1545-8830 online
DOI: 10.1080/0740817X.2012.689125

Fairing the gamma: an engineering approach to sensitivity estimation

WANMO KANG[1], KYOUNG-KUK KIM[2] and HAYONG SHIN[2,*]

[1]*Department of Mathematical Sciences, KAIST, Dajeon, South Korea*
[2]*Department of Industrial and Systems Engineering, KAIST, Daejeon, South Korea*
E-mail: hyshin@kaist.ac.kr

Received October 2011 and accepted March 2012

In the finance industry, obtaining stable estimates for sensitivities of derivatives to price changes in an underlying asset is very important from a practical point of view. However, this aim is often hindered by the absence of closed-form expressions for Greeks or the requirement of an excessive computational workload due to the complexities of various exotic derivative structures. However, *ad hoc* numerical schemes to produce stable Greeks such as nonlinear regression can result in nonsensical values. This article proposes a fairing algorithm designed for the computation of gamma values of exotic derivatives. Examples are presented at exotic derivatives to which the algorithm is applied and some analytical and numerical results are provided that show its usefulness in reducing the mean square error of gamma estimates.

Keywords: Sensitivities, Monte Carlo estimation, fairing

1. Introduction

To any participant in the financial derivatives markets, the sensitivities of derivative products in her portfolio are indispensable data for hedging the market risks to which the portfolio is exposed. Moreover, it is important to have these so-called Greeks that are reasonably good and stable in a sense to be made more precise. Several methods to address this issue have been proposed that have had mixed degrees of success depending on the payoff structures of the derivatives. To name just a few of the methods, a Finite Difference (FD) scheme is well summarized in Glasserman (2004), a pathwise method and a likelihood ratio method were proposed by Broadie and Glasserman (1996), and a Malliavin calculus-based method was developed in Fournié *et al.* (1999) and Fournié *et al.* (2001). And it is well known that, in many cases, FD schemes are less reliable than other methods when applicable. However, depending on the particular products of interest, we often have to resort to an FD scheme because of failed regularity conditions (on payoff functions or on underlying stochastic processes) or because of final formulae that might be formidable to draw or difficult to implement even when all conditions are satisfied.

For example, let us consider the following equity-linked security whose underlying assets are S^1 and S^2. We call this product ELS2 to emphasize its dependence on two equity prices. The payoff is basically a function of the minimum of two ratios S_t^i/S_0^i; that is,

$$\hat{S}_t = \min\left\{\frac{S_t^1}{S_0^1}, \frac{S_t^2}{S_0^2}\right\}, \quad t \in [0, T],$$

where S_t^i is the price of asset i at time t and T indicates the maturity, and we have six early redemption dates $t_i = iT/6$, $i = 1, \ldots, 6$, with redemption thresholds $l_i > 0$. In early redemption the contract ends at time t_i if a certain condition on $\hat{S}$ is met at that time. More specifically,

- if $\hat{S}_{t_i} > l_i$ for some i for the first time, then the contract expires at time t_i with payoff $1 + r_i$ to the investor;
- if there was no early redemption and $\min\{\hat{S}_t : 0 \le t \le T\} > b$, the payoff is one;
- the final payoff is $\hat{S}_T$ otherwise.

Here $\min\{\hat{S}_t : 0 \le t \le T\}$ is the minimum of daily closing prices until maturity and b is the value of the lower knock-in barrier. The computation of Greeks for this product is non-trivial by any of the existing methods for sensitivity estimation. ELS2 is a typical kind of equity derivative actively traded on Korean financial markets. Many financial contracts, indeed, contain payoffs as complexly structured as this example.

*Corresponding author
Color versions of one or more of the figures in the article can be found online at www.tandfonline.com/uiie.

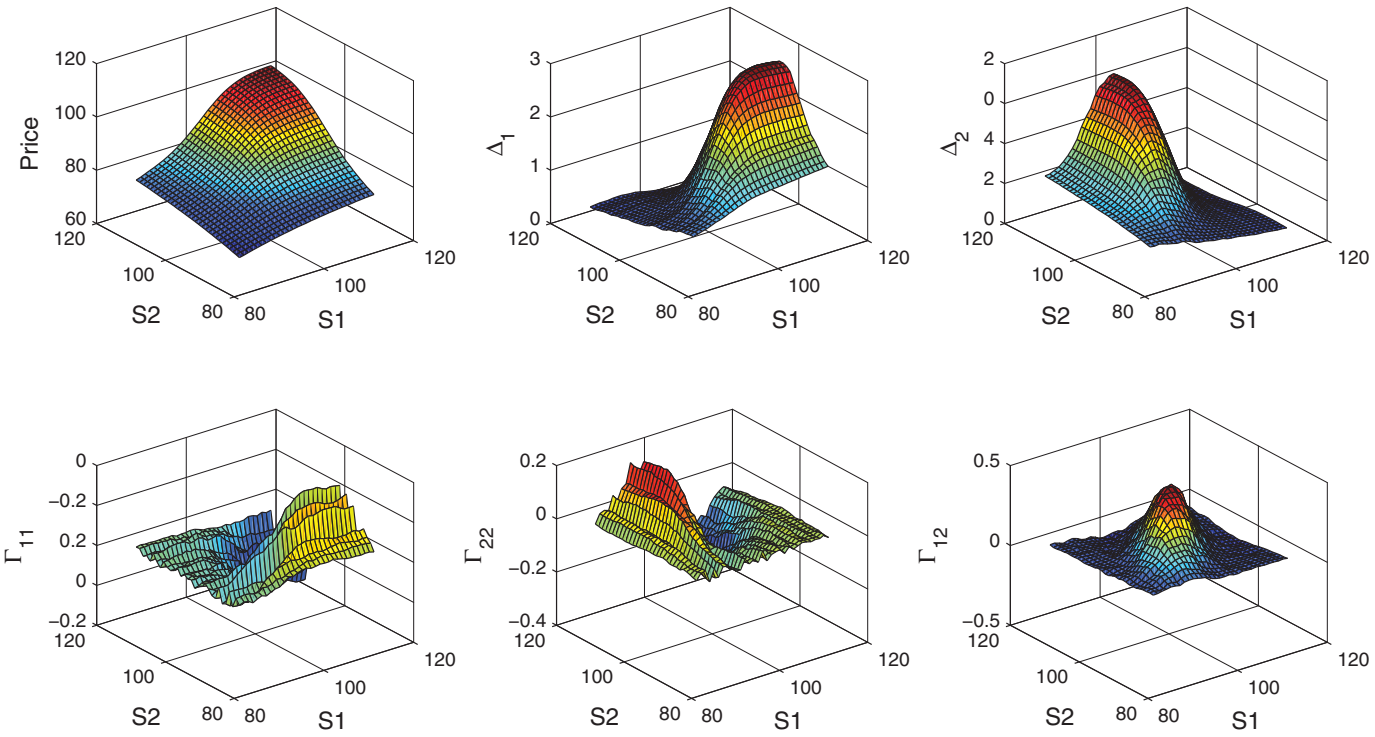

Fig. 1. Price, delta, and gamma surfaces for ELS2 obtained using a FD scheme.

There are many payoff features that can be easily incorporated into any derivative contract. Simple examples include digital and barrier features as in ELS2. If derivative products in a portfolio consist of various combinations of such payoff features, then each combination might easily require a separate Greek calculation code to employ non-FD methods. (In this article, we focus on sensitivities with respect to the underlying stock price up to the second degree.) In addition, one needs to run the code at each parameter value in a certain range where the user wants to see Greeks for the purpose of risk management. (One exception is Giles and Glasserman (2006), where the authors provide a variant of the pathwise method that gives multiple Greeks at once.)

However, if one wants to implement an FD scheme, a notable practical difficulty arises. Namely, the sensitivity estimates become quite unstable especially when we take higher-order sensitivities such as gammas. Figure 1 shows the prices, deltas, and gammas for ELS2 computed by an FD scheme in a rectangular range. Geometric Brownian motions were assumed as the underlying asset price processes. It is clear that the gammas fluctuate much wider than the prices and the deltas. This instability has been one of the big barriers in the implementation of Monte Carlo methods in practice because it is essential to have a robust way of calculating Greeks in a financial firm where computations of Greeks need to be automated and various derivatives portfolios are managed. This article is an attempt to address some computational issues that appear in applying FD schemes to sensitivity estimates for derivatives that involve severe costs in implementing non-FD methods. For a related work by the authors, we refer the reader to Kang *et al.* (2012).

Now, we briefly summarize our approach to delta and gamma computations using Monte Carlo simulation. First, we assume that a Monte Carlo method provides price estimates at a set of initial asset values. They are given in the form of confidence intervals or pairs of sample means and sample variances from the Monte Carlo runs. Thus, we work with a sequence of intervals in the case of a derivative on a single underlying asset or an array of intervals for two underlying assets. We can safely assume that model parameters except asset prices stay at their estimated values during a few hours or a single trading day. Hence, once we compute Greeks in a range of asset prices, hedging operations can be performed based on these values. The "circuit breaker" in each exchange provides a natural range for this preparatory Greek computation.

Starting with a set of sample means, we apply *fairing* iterations to these values within fixed intervals that, throughout this article, we set as being centered at sample means with a half-width equal to one or one half times sample standard errors. Then, we apply the ordinary FD scheme for delta and gamma computations after the fairing algorithm stops according to a certain stopping condition. This stopping condition will be detailed in a later section. Hence, fairing

iterations can be uniformly applied to derivatives with any type of payoff functions or to any specification of stochastic models.

Fairing is a Computer-Aided Design (CAD) technology developed originally in the automotive industry to obtain a surface with a smoother curvature distribution for high-quality machining and aesthetic body shapes of vehicles. Under the condition that the value function under consideration is twice continuously differentiable with respect to underlying assets prices, our new fairing approach is applicable. We provide some motivating examples in Section 2. A detailed procedure is presented in Section 3. Section 4 exhibits numerical test results and Section 5 deals with some analysis results for the method. We conclude in Section 6.

2. Motivation

Let $Y(\theta)$ be the payoff of interest where θ is a parameter. The price is given by $E[Y(\theta)]$ under some probability measure P. We set

$$\alpha(\theta) = E[Y(\theta)]. \tag{1}$$

We are looking for $\alpha'(\theta)$ and $\alpha''(\theta)$ where θ varies in a certain range. In this article, θ is set to be the underlying stock price. In addition to the difficulties of applying existing methods for those mathematical derivatives, it is often out of practical concerns that we are interested in computing *discrete delta* and *discrete gamma* at given points $\{\theta_1, \ldots, \theta_n\}$. See, e.g., Taleb (1997) on discrete rebalancing. We assume that the points are equally spaced, say $h = \theta_{i+1} - \theta_i$ for each i. The discrete delta (Δ_i) and gamma (Γ_i) for $i = 1, \ldots, n-1$ are then defined by

$$\Delta_i = \frac{\alpha(\theta_{i+1}) - \alpha(\theta_{i-1})}{2h},$$
$$\Gamma_i = \frac{\alpha(\theta_{i+1}) - 2\alpha(\theta_i) + \alpha(\theta_{i-1})}{h^2}.$$

We denote the Monte Carlo estimate at θ with m simulation trials by $\overline{Y}_m(\theta)$. Then, the corresponding estimates of discrete delta and gamma become

$$\widehat{\Delta}_i = \frac{\overline{Y}_m(\theta_{i+1}) - \overline{Y}_m(\theta_{i-1})}{2h}, \tag{2}$$
$$\widehat{\Gamma}_i = \frac{\overline{Y}_m(\theta_{i+1}) - 2\overline{Y}_m(\theta_i) + \overline{Y}_m(\theta_{i-1})}{h^2}. \tag{3}$$

These estimates can be regarded as the FD approximations to the instantaneous delta and gamma values. To motivate our approach, let us consider some examples that illustrate the difficulties in obtaining reliable Greek estimates via FD schemes. Throughout this article, we consider the following four contracts with varying degrees of exoticness

- CO: vanilla European call option (strike $K = 100$ and maturity $T = 4$).
- DO: cash-or-nothing digital option ($K = 100$, $T = 4$, payoff = 0 or 10).
- ELS1: structured security linked to the performance of an underlying equity with early redemption features and down barrier feature. This product can be characterized by many discontinuities in the payoff structure. Details of the payment plan of this product are same as those of ELS2 introduced in Section 1. The only difference is that the worst performer is replaced by the normalized price of the single underlying equity. In numerical experiments, we work with parameters $T = 1$ year, $l_1 = l_2 = 0.95$, $l_3 = l_4 = 0.9$, $l_5 = l_6 = 0.85$, $r_i = 0.05 \times i$, and, finally, $b = 0.7$.
- ELS2: Explained in Section 1 and the parameters are the same as in ELS1.

The Black–Scholes model is used in the experiments; however, it should be noted that our approach is independent of any model specification, as becomes clear in the subsequent section. As for CO and DO, we use the Black–Scholes formulae to compute the true prices. As there is no analytic or semi-analytic formula available for ELS1 or ELS2, Monte Carlo estimates with a billion simulation trials are used as the true prices. The price curves from

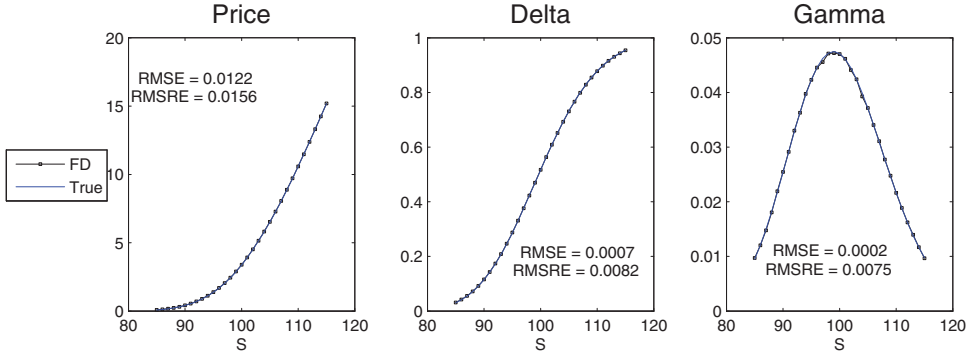

Fig. 2. Price/delta/gamma of CO.

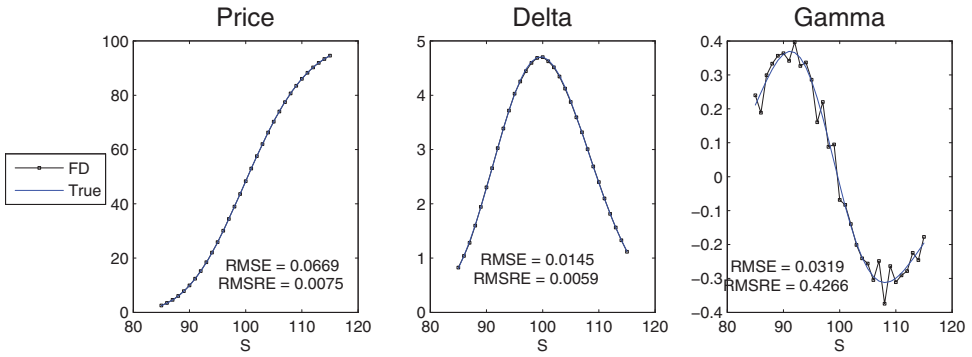

Fig. 3. Price/delta/gamma of DO.

simulation with 10^5 paths as well as the true curves are plotted in Figs. 2 to 4 for comparison. Volatility levels in those figures are fixed at 30%. Also, in Fig. 4, the time-to-maturity is 4 weeks, which is the same as CO and DO. Lastly, we note that the antithetic variable and the common random technique are employed.

As a measure of the goodness of estimates, we consider Root Mean Squared Error (RMSE) and Root Mean Squared Relative Error (RMSRE). If $\hat{\alpha}_i$ and α_i denote the estimated value and the true value, respectively, then these measures are defined as

$$\text{RMSE} = \sqrt{\sum_{i=0}^{n}(\hat{\alpha}_i - \alpha_i)^2} \quad \text{and}$$

$$\text{RMSRE} = \sqrt{\sum_{i=0}^{n}\left(\frac{\hat{\alpha}_i - \alpha_i}{\tilde{\alpha}_i}\right)^2}, \tag{4}$$

where $\tilde{\alpha}_i = \max\{|\alpha_i|, 10^{-3}(n+1)^{-1}\sum_{j=0}^{n}|\alpha_j|\}$. The reason for the introduction of $\tilde{\alpha}_i$ is that, otherwise, it may exaggerate the error when the true value is too small. However, there is a possibility to have large RMSRE values when α_i values are very small. Indeed, this is what we observe in some of numerical tests reported below. However, usually small true values do not cause problems in actual trading operations.

For the standard European call option (Fig. 2) whose payoff function is continuous, all three curves (price, delta, and even gamma curve) are quite close to the true ones. For the digital option with cash or not payoff (Fig. 3), the gamma curve reveals a jigsaw shape. For ELS1 (Fig. 4), it is highly unstable. Actually, even the delta curve deviates from the true one under different conditions such as fewer samples, longer maturity, or higher asset volatility.

Certainly, high fluctuations in gamma estimates are undesirable in terms of dynamic hedging of financial derivatives. Now, recall that, as said in the Introduction, a risk manager or a trader might want to pre-compute relevant Greek values and retrieve appropriate numbers during the day to enhance operational efficiency. Our approach is based on the utilization of price estimates at different parameter values as well as the interval estimates (i.e., $(1-\beta)$ confidence intervals):

$$\left(\overline{Y}_m(\theta_i) - z_{\beta/2}\frac{\hat{s}_m(\theta_i)}{\sqrt{n}},\ \overline{Y}_m(\theta_i) + z_{\beta/2}\frac{\hat{s}_m(\theta_i)}{\sqrt{m}}\right),$$

where $\hat{s}_m(\theta) = \sqrt{(m-1)^{-1}\sum_{i=1}^{m}(Y_i(\theta) - \overline{Y}_m(\theta))^2}$. Basically, we use this extra information by allowing some

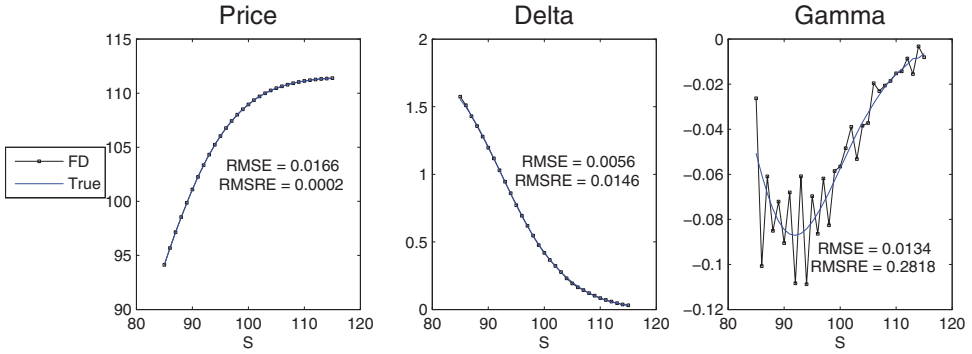

Fig. 4. Price/delta/gamma of ELS1.

flexibility in choosing the values for the FD scheme. Let us fix a positive constant δ to determine the width of intervals from which input values, say p_i, for finite differencing are chosen:

$$I_i = \left(\overline{Y}_m(\theta_i) - \delta \frac{\hat{s}_m(\theta_i)}{\sqrt{m}},\ \overline{Y}_m(\theta_i) + \delta \frac{\hat{s}_m(\theta_i)}{\sqrt{m}} \right). \tag{5}$$

We then put these p_i values in place of $\overline{Y}_m(\theta_i)$ in Equations (2) and (3) to *fair* the Greek curves and obtain

$$\widehat{\Delta}_i(\mathbf{p}) = \frac{p_{i+1} - p_{i-1}}{2h}, \tag{6}$$

$$\widehat{\Gamma}_i(\mathbf{p}) = \frac{p_{i+1} - 2p_i + p_{i-1}}{h^2} \tag{7}$$

for $i = 1, \ldots, n-1$, and call them the Greek estimates for $\mathbf{p} = (p_0, \ldots, p_n)$. We often call $\mathbf{p}$ a curve, meaning the piecewise linear curve connecting $\{(\theta_i, p_i) : i = 0, \ldots, n\}$.

Before we move onto the next section, let us discuss some numerical implications of I_i. In the case of ELS1, 10^4 sample paths yield 0.01 to 0.11 USD of standard errors for the price range taken in the test. This is less than 0.12% of the share price. (The number is reduced to 0.04% for 10^5 paths.) Actually, the modified p_i via the algorithm in Section 3 are only within -0.1 to 0.03% (for 10^4 runs) and -0.011 to 0.018% (for 10^5 runs) from the original price estimates.

3. Curve/surface fairing

Facing the question in Section 2 about how to enhance the gamma estimates, the following techniques seem to be two natural approaches to the main problem that arises due to the undesirable heavy fluctuations of Greek estimates; first, signal processing techniques based on Fourier analysis and, second, curve fairing techniques developed in the geometry processing community, such as CAD. In this article, we explore the avenue of curve fairing techniques.

In general, curve fairing is a method of changing the original curve by only a small amount to obtain a new curve with more appealing characteristics. A fast growing research area in CAD is the "digital shape reconstruction" (formerly called reverse engineering) field, which deals with constructing a mathematical representation of the shape from the measured data of a physical object possibly with measurement noise; e.g., Salvi and Várady (2005). An essential step in digital shape reconstruction is fairing, which is also referred to as de-noising. (Some researchers argue that de-noising is different from fairing in its problem formulation; e.g., Sun *et al.* (2008).) The goal of fairing in digital shape reconstruction is to remove possible noises under the assumption that the original curve (or surface) is smooth. Although this goal is perfectly in sync with our needs, to the best of our knowledge there is no literature applying this technique to the computation of prices and hedging parameters of financial products. Among various fairing algorithms, we start with a simple one proposed by Cho and Choi (2001) and modify it to fit with our problem. For the variety of alternative fairing algorithms, we refer the reader to Sapidis and Farin (1990), Eck and Jaspert (1994), Yamada *et al.* (1999), and Zhang *et al.* (2001).

Recall that the true function is $\alpha(\theta) = E[Y(\theta)]$ and we assume that $\alpha(\theta)$ is a smooth function of parameter θ. At each θ_i, I_i defined by Equation (5) is a modified confidence interval for $\alpha(\theta_i)$. Greek estimates such as delta or gamma are defined by Equations (6) and (7) for original Monte Carlo estimates or values obtained via fairing. As will be seen later, delta estimates after fairing exhibit smoother shapes even though our primary focus is on gamma estimates.

3.1. *Local fairing formula for internal points*

In order to obtain a curve with smooth gamma values, it is desirable to have gradual changes of $\hat{\Gamma}_i(\mathbf{p})$ in i. Thus, we define the local fairness measure of a price curve $\mathbf{p}$ at θ_i as

$$\begin{aligned} \varepsilon_i(\mathbf{p}) &= |(\hat{\Gamma}_{i+1}(\mathbf{p}) - \hat{\Gamma}_i(\mathbf{p})) - (\hat{\Gamma}_i(\mathbf{p}) - \hat{\Gamma}_{i-1}(\mathbf{p}))| \\ &= \frac{|p_{i+2} - 4p_{i+1} + 6p_i - 4p_{i-1} + p_{i-2}|}{h^2}. \end{aligned} \tag{8}$$

(Note that $\varepsilon_i(\mathbf{p})$ is actually a measure of "unfairness." However, we will follow the terminology in the curve fairing literature such as Eck and Jaspert (1994), Cho and Choi (2001), and many others.) Minimizing $\varepsilon_i(\mathbf{p})$ becomes optimal when we move $\hat{\Gamma}_i(\mathbf{p})$ to the average of $\hat{\Gamma}_{i-1}(\mathbf{p})$ and $\hat{\Gamma}_{i+1}(\mathbf{p})$ (see Fig. 5), which in turn yields the optimal position of p_i as

$$\begin{aligned} p_i^* &= \frac{1}{3}(4m_1 - m_2) \ \text{ where } \ m_1 = \frac{1}{2}(p_{i+1} + p_{i-1}), \\ m_2 &= \frac{1}{2}(p_{i+2} + p_{i-2}). \end{aligned} \tag{9}$$

Hence, the optimal position of p_i can be interpreted as the 1:4 extrapolation point between the mid-point of the first-order neighbors $p_{i\pm1}$ and the mid-point of the second-order neighbors $p_{i\pm2}$, as shown in Fig. 6.

3.2. *Considerations for boundary points*

There are various ways of imposing boundary conditions, including local approximations such as cubic curve fitting. However, extensive numerical tests suggested that there is no single method that performs well when compared with the naïve one, which fixes four boundary points

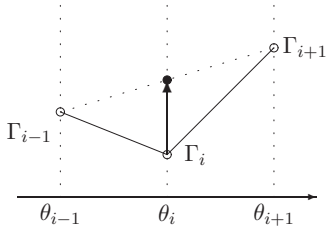

Fig. 5. Optimal position among three points.

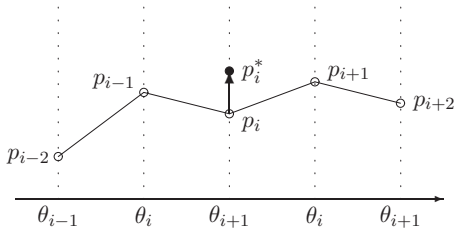

Fig. 6. Optimal position among five points.

p_0, p_1, p_{n-1}, p_n at the original price estimates. Hence, in our numerical implementation, we fix those boundary points.

3.3. *Fairing algorithm*

Now, we are ready to describe the algorithm for curve fairing. We begin with the initial discrete price curve $\mathbf{p}_0 = \{p_i : i = 0, \ldots, n\}$. Let $\mathbf{p}_k = \{p_{i,k} : i = 0, \ldots, n\}$ denote the discrete curve obtained after the kth iteration. We compute $\mathbf{p}_k$ by applying the local fairing formula (9) to $\mathbf{p}_{k-1}$; i.e., $p_{i,k+1} = p^*_{i,k}$ with $p_{i,0} = p_i$. However, this simple setting is modified to reflect the following two concerns.

Damping factor: Blind application of the local fairing scheme may result in oscillations as shown in Fig. 7. This can be explained by an analogy to a swinging pendulum without any resistance, which will swing forever. To avoid this situation, a damping factor is introduced. Let $v_i = p^*_{i,k} - p_{i,k}$. Then the new position becomes $p_{i,k+1} = p_{i,k} + \tau v_i$, where $\tau \in [0, 1]$ is the damping factor. If we use a large value for τ (near one), resulting curves from each iteration become unstable, whereas small τ (near zero) results in slow convergence. From numerical tests, we found that $\tau = 0.5$ gives a reasonable convergence speed. More detailed analysis is done in Section 5. The reader is referred to, for example, Cho and Choi (2001) for additional discussions regarding damping factors.

Fairing tolerance: Equation (9) may give optimal points that are far from the original ones. Since it is desirable that altered price estimates from fairing are still good reference values for true prices, we confine the movement of each data point p_i to I_i where δ is the fairing tolerance; i.e., $|p_{i,k} - p_i| < \delta \hat{s}_n(\theta_i)/\sqrt{n}$. In our numerical tests, we use $\delta = 1$ so that each $p_{i,k}$ stays within one standard error from p_i. Combining the above two issues, we get the following iterative algorithm:

```
Algorithm Gamma_Curve_Fairing
do {
      for i = 2 to n − 2 {
        compute p*_{i,k} using (9);
         v_i = p*_{i,k} − p_{i,k};
         w_i = p_{i,k} + τ v_i − p_i :
               if w_i > δ ŝ_n(θ_i)/√n, then w_i = δ ŝ_n
               (θ_i)/√n;
               if w_i < −δ ŝ_n(θ_i)/√n, then w_i =
               −δ ŝ_n(θ_i)/√n;
         p_{i,k+1} = p_i + w_i;
      }
} while (stopping condition is not met)
```

3.4. *Stopping condition*

The remaining question is when to stop the iteration in the algorithm. Figure 8 shows the change in gamma curves of DO as the number of iterations increases. Notice that too many fairing iterations could be harmful, resulting in somewhat flattened gamma curves.

Fairness of a curve may have different meanings in different applications, depending on the requirements as discussed in Salvi and Várady (2005). For the discretely represented curve as we have in our problem, we will follow the suggestion in Eck and Jaspert (1994), where the global fairness of a curve is defined by $\varepsilon = \sum(\kappa_i'')^2$ where κ_i is the curvature of the curve at θ_i. As it is not straightforward to define the term κ_i'' for a discrete curve, we approximate κ_i'' in the same way that we approximate κ_i by $\hat{\Gamma}_i(\mathbf{p})$, the second-order difference of price estimates. In other words, using $\hat{\Gamma}_i(\mathbf{p})$, we set

$$\begin{aligned}\varepsilon(\mathbf{p}) &= \sum_i ((\hat{\Gamma}_{i+1}(\mathbf{p}) - \hat{\Gamma}_i(\mathbf{p})) - (\hat{\Gamma}_i(\mathbf{p}) - \hat{\Gamma}_{i-1}(\mathbf{p})))^2 \\ &= \sum_i \varepsilon_i(\mathbf{p})^2,\end{aligned}$$

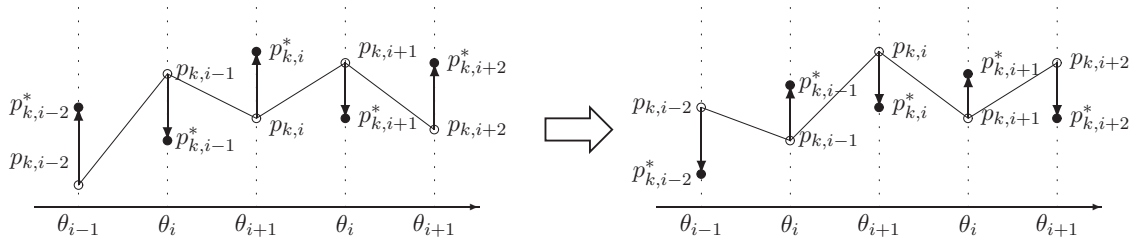

Fig. 7. Oscillations in fairing iterations.

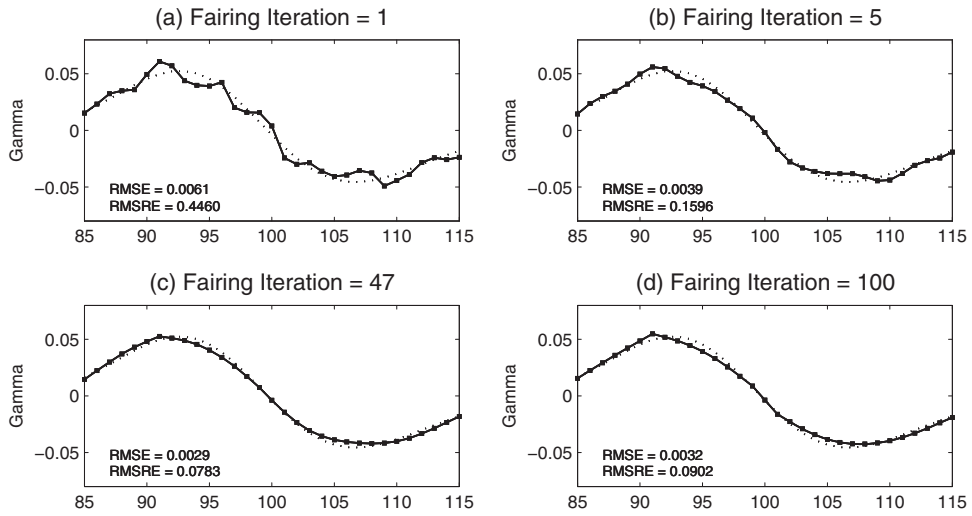

Fig. 8. Evolution of gamma curves.

where $\varepsilon_i(\mathbf{p})$ is the local fairness defined in Equation (8). With this global fairness measure, we continue the fairing algorithm in Section 3.3 while $\varepsilon(\mathbf{p})$ is decreasing or while the ratio of measurements from two consecutive iterations is larger than some threshold value. Table 1 shows the global fairness measurements for the original price curve, the output of the fairing algorithm, and the true price curve. All necessary parameter specifications are explained in Section 4.

3.5. *Extension to surface fairing*

The curve fairing algorithm above can be easily modified for a price surface that consists of a two-dimensional array of data points. The relevant parameters are, then, the underlying asset prices (θ^1, θ^2). Since each true price $\alpha(\theta_i^1, \theta_j^2)$ on the price surface is located on two cross-sectional curves $\alpha(\theta_i^1, \cdot)$ and $\alpha(\cdot, \theta_j^2)$, we can apply the curve fairing technique independently and then the two resulting positions are averaged. We will omit the details of surface fairing since the reader can easily follow the main idea.

Table 1. Reduction of fairness measures for ELS2, number of sample paths $= 10^5$

	Fairness measure		
Maturity	*None*	*Fairing*	*True*
1M	0.701 971	0.128 094	0.089 540
3M	1.208 936	0.110 894	0.023 177
5M	1.448 335	0.095 314	0.013 826
7M	1.670 309	0.086 091	0.018 881
9M	1.436 607	0.061 357	0.010 141
11M	1.722 928	0.036 982	0.012 825

4. Numerical tests

We conducted numerical experiments on the performance of the fairing algorithm, focusing on four contingent claims (CO, DO, ELS1, and ELS2) whose payoff structures were described in Section 2. The asset price dynamics of interest was assumed to follow a geometric Brownian motion. Other parameters used in the tests are as follows: for CO and DO, we fixed the maturity equal to 4 weeks and varied the level of asset volatility from 10% to 50% with a step size of 10% while for the other two contracts we fixed the volatility parameters and correlation level (volatility 30% for ELS1, 30% and 40% for the two assets in ELS2 with correlation 0.6) and varied the maturities from 1 month to 11 months. Even though we do not report it here, the performance of the algorithm for ELS1 and ELS2 turned out to be very similar for different volatility and correlation specifications.

For the benchmark values to be compared with algorithm outputs, analytical closed-form formulae for CO and DO were used; however, for the other two exotic securities, we used the values obtained from a billion simulation trials. For all contracts, 10^4, 10^5, and 10^6 simulated paths were used to produce price and Greek estimates.

Results are listed in Tables A1 to A12 in Appendix A. Recall that we constructed delta and gamma curves or surfaces by applying an FD scheme to price estimates from the usual Monte Carlo computations. The range of the parameter θ was $\{84, \ldots, 116\}$. Therefore, we computed delta and gamma estimates for $\theta \in \{85, \ldots, 115\}$. Through fairing, new price estimates or, put differently, new price curves or surfaces were generated, which in turn yielded new delta and gamma curves or surfaces. The performance measures employed were RMSE and RMSRE as in Equation (4). The effectiveness of fairing is essentially captured by the

ratios of these measures from the original FD estimates and the faired estimates.

There are three main observations that can be made. First, we do not see much improvement for CO where the ratios for price/delta/gamma are greater than one in several places and close to one even when they are less than one. However, the results improve quite a bit as discontinuities start to kick in. Second, we see much better performance for gammas rather than prices or deltas. Intuitively, this can be understood as a result of the fairness measure that we are using to smooth gamma estimates. Finally, if we closely look at the RMSEs of gamma values from the faired estimates with 10^4 sample paths, then the numbers mostly lie somewhere between the RMSEs of gamma values from the original Monte Carlo estimates with 10^5 (Table A10) and 10^6 (Table A12) sample paths. Consequently, at least for securities covered in this article, it is seen that the algorithm performs better for more exotic securities and for gamma estimates. In addition, the computational savings seem to be between 10 and 100 times, which is remarkable considering that the processing time for the algorithm is negligible, not to mention the ease of coding.

Now, Figs. A1 to A3 in Appendix A present how the original gamma curves for CO, DO, and ELS1 are changed after fairing. We do this only for gamma curves as the improvement for price/delta estimates is not as much as gamma estimates. For Fig. A1, the asset volatility is set equal to 30%. We note that the fluctuations of gammas are mitigated after fairing. The other figures depict price/Greek estimates corresponding to ELS2 with 10^5 trials. To see the changes from the original values, Fig. A4 needs to be compared with Fig. 1. Figure A5 amplifies this for Γ_{11} for the reader's convenience.

Remark 1. We observe very large RMSRE values in some parts of the tables; see, e.g., return on the gamma values of Tables A4 to A6. Even though RMSRE works fine most of the time, it can return an absurdly large value when a true value is very close to zero. This feature of the RMSRE can lead to somewhat strange behavior in the outcomes, but such small values do not lead to practical concerns.

5. Analysis of fairing

In this section, we give some analytical and numerical results that support the use of fairing in the Monte Carlo simulation context. To this end, let us assume that we have point estimates p_i for the unknown function values $\alpha_i = \alpha(i/n)$ for $i = 0, \ldots, n$; i.e., $\theta_i = i/n$ where $\alpha(\cdot)$ is defined as in Equation (1). We deliberately focus on analyzing the effects of the first iteration of fairing on the mean square error of gamma estimates. This is to obtain some intuition about the method without becoming lost in the analysis, which becomes extremely complicated as further iterations are performed. For notational convenience, we set $p_i = p_{i,0} = \overline{Y}_m(i/n)$.

In Section 5.1, we deal with the case where the p_i are independent of each other. This happens when we do not employ the common random number technique. Even though this technique is frequently used and thus the analysis in the subsection does not apply in such a case, it greatly simplifies computations and yields analytical results. In Section 5.2, we investigate how a correlation structure between the p_i is generated via simple examples and conduct a numerical experiment to see how correlation structures affect the performance of the algorithm.

5.1. *Independent case*

Throughout this subsection, we assume that $Z_i := p_i - \alpha_i$ are independent and identically distributed as $\mathcal{N}(0, \sigma^2)$. The assumption of normal distribution is not harmful as long as the number of simulation trials is large enough. However, the same variance σ^2 at all points is not guaranteed because the variance $E[(Y(i/n) - \alpha_i)^2]$ depends on the $Y(\cdot)$, which could be quite different from point to point. Nevertheless, we can consider this σ^2 as a sort of maximal possible variance that point estimates p_i have, so that we can see how fairing works even in the worst case. Regarding the independence, we deal with the correlated p_i case in the following section. However, at least it should be noted that this correlation structure of the p_i is quite different from a perfect correlation case as long as the payoff function has exotic features. For this reason and for the analytical tractability, the independence assumption on the Z_i is imposed.

Let us denote the vector $(-1/6, 2/3, -1, 2/3, -1/6)$ by $\boldsymbol{\varphi}$. Then, from the definition of p_i^* in Equation (9), we obtain

$$\begin{aligned} p_i^* - p_i &= \frac{4(p_{i+1} + p_{i-1})}{6} - \frac{p_{i+2} + p_{i-2}}{6} - p_i \\ &= -\Lambda_i h^4 + \boldsymbol{\varphi} \times \mathbf{Z}_i \end{aligned}$$

for the interior points ($i = 2, \ldots, n-2$) where $h = n^{-1}$, $\mathbf{Z}_i = (Z_{i-2}, \ldots, Z_{i+2})$, and

$$\Lambda_i = \frac{1}{h^4}\left(\frac{1}{6}\alpha_{i+2} - \frac{2}{3}\alpha_{i+1} + \alpha_i - \frac{2}{3}\alpha_{i-1} + \frac{1}{6}\alpha_{i-2}\right).$$

If we write Γ_i for the approximate value of the second-order derivative of the function $\alpha(\cdot)$ using to finite difference, then Λ_i can be written as $h^{-2}(\Gamma_{i+1} - 2\Gamma_i + \Gamma_{i-1})$, which is an approximate value for the fourth-order derivative of $\alpha(\cdot)$ at θ_i. After the first iteration, we get

$$\begin{aligned} p_{i,1} &= p_i + g(\tau(p_i^* - p_i)), \quad \text{where} \\ g(x) &= x\mathbf{1}_{\{|x| \le \delta\sigma\}} + \delta\sigma\mathbf{1}_{\{x > \delta\sigma\}} - \delta\sigma\mathbf{1}_{\{x < -\delta\sigma\}}. \end{aligned}$$

Recall that τ and δ stand for the damping factor and the fairing tolerance, respectively. Then, finally, we have the estimates for the Γ_i from fairing: $\Gamma_{i,1} = h^{-2}(p_{i+1,1} - 2p_{i,1} + p_{i-1,1})$.

As a measure of goodness of the estimates $\Gamma_{i,1}$, we use the Mean Square Error (MSE):

$$\frac{1}{n-1}\sum_{i=1}^{n-1} E[(\Gamma_{i,1}-\Gamma_i)^2], \tag{10}$$

as n increases. Note that this MSE can be rewritten as

$$\begin{aligned}
&\frac{1}{n-1}\sum_{i=3}^{n-3} E[(\Gamma_{i,1}-\Gamma_i)^2] \\
&\quad= \frac{1}{(n-1)h^4}\sum_{i=3}^{n-3} E[(p_{i+1,1}-2p_{i,1}+p_{i-1,1} \\
&\qquad -(\alpha_{i+1}-2\alpha_i+\alpha_{i-1}))^2] \\
&\quad= \frac{1}{(n-1)h^4}\sum_{i=3}^{n-3} E[(\tilde{A}_{i+1}-2\tilde{A}_i+\tilde{A}_{i-1})^2]
\end{aligned}$$

plus the sum of the summands at $i = 1, 2, n-2, n-1$, where $\tilde{A}_i = Z_i + g(-\tau\Lambda_i h^4 + \tau\boldsymbol{\varphi}\times\mathbf{Z}_i)$. The first two terms and the last two terms are treated separately because they involve $p_{i,1}$ obtained from the fairing algorithm at boundary points. The next proposition gives us an upper bound that is more amenable to analysis than the MSE itself.

Lemma 1. *The MSE (10) is bounded by*

$$\frac{1}{(n-1)h^4}\sum_{i=3}^{n-3} E\left[(A_{i+1}-2A_i+A_{i-1})^2\right],$$

where $A_i = Z_i + g(\tau\boldsymbol{\varphi}\times\mathbf{Z}_i)$*, plus extra terms:*

$$\begin{aligned}
&\frac{1}{(n-1)h^4}\sum_{i=3}^{n-3}\left[4\sigma\left(\sqrt{\frac{3}{\pi}}+2\delta\right)\zeta_i+\zeta_i^2\right] \\
&\qquad+\frac{4\sigma^2}{(n-1)h^4}\left[16\delta^2+16\delta\sqrt{\frac{3}{\pi}}+6\right],
\end{aligned}$$

with $\zeta_i = |\tau\Lambda_{i+1}h^4| \wedge (\delta\sigma) + 2|\tau\Lambda_i h^4| \wedge (\delta\sigma) + |\tau\Lambda_{i-1}h^4| \wedge (\delta\sigma)$.

Proof. See Appendix B. ■

We aim to compare the MSE (10) with the MSE for $\widehat{\Gamma}_i$, which is the estimate for Γ_i with no fairing algorithm applied. The latter is easily shown to be $6\sigma^2/h^4$. Then, the extra terms in the above lemma can be considered negligible for all large values of n when divided by $6\sigma^2/h^4$. Indeed, if $\max_{t\in[0,1]}|\alpha''(t)|$ is well defined and finite, then each $|\Lambda_i h^4| = h^2|\Gamma_{i+1} - 2\Gamma_i + \Gamma_{i-1}|$ is bounded by Kh^2 for some constant K because $(\alpha_{i+1}-2\alpha_i+\alpha_{i-1})/h^2$ converges as h decreases. Hence, the first term is $O(h^2)$. Moreover, if $\alpha(\cdot)$ has bounded fourth derivatives on [0, 1], then by a similar observation we have that this term is $O(h^4)$. The second one in the extra terms is clearly $O(h)$. Consequently, it is enough to consider

$$\frac{1}{6(n-1)\sigma^2}\sum_{i=3}^{n-3} E\left[(A_{i+1}-2A_i+A_{i-1})^2\right] \tag{11}$$

to measure the performance of fairing algorithm on the MSE of gamma estimates approximately.

Proposition 1. *The quantity (11) is given by* $(n-5)/(n-1)$ *times.*

$$\begin{aligned}
&1+\delta^2 P(|Y|>x) - \frac{2\sqrt{70}\delta}{3}E[Y;\, Y>x] \\
&\quad+\frac{35\tau(\tau-2)}{18}E\left[Y^2;\,|Y|\le x\right] \\
&\quad+\frac{2\delta^2}{3}P(Y>x,\,Y'>x) - \frac{2\delta^2}{3}P(Y>x,\,Y'<-x) \\
&\quad+\frac{2\sqrt{70}\tau\delta}{9}E[Y;\,|Y|\le x,\,Y'>x] \\
&\quad+\frac{35\tau^2}{54}E[YY';\,|Y|\le x,\,|Y'|\le x] \\
&\quad-\frac{8\delta^2}{3}P(Y>x,\,Y''>x) + \frac{8\delta^2}{3}P(Y>x,\,Y''<-x) \\
&\quad-\frac{8\sqrt{70}\tau\delta}{9}E[Y;\,|Y|\le x,\,Y''>x] \\
&\quad-\frac{70\tau^2}{27}E[YY'';\,|Y|\le x,\,|Y''|\le x],
\end{aligned} \tag{12}$$

where $x = 6\delta/(\sqrt{70}\tau)$ *and* Y, Y', Y'' *are correlated standard normal random variables with* $\mathsf{Corr}(Y, Y') = 0.4$ *and* $\mathsf{Corr}(Y, Y'') = -0.8$.

Proof. See Appendix B. ■

Numerical implementation of Equation (12) can be done using softwares such as MATLAB, which contains Probability Density Functions (PDFs) and Cumulative Distribution Functions (CDFs) for standard normal random variables and multivariate normal random variables. For the terms that involve Y only, we can further simplify them using the following formulae:

$$\begin{aligned}
E[Y;\,Y>x] &= \phi(x), \\
E[Y^2;\,|Y|\le x] &= -2x\phi(x) + 2\Phi(x) - 1,
\end{aligned}$$

where $\phi(\cdot)$ and $\Phi(\cdot)$ are the PDF and the CDF of a standard normal.

Results of numerical experiments are shown in Fig. 9. The graphs exhibit the behavior of this function depending on δ and τ. We can see the effectiveness of the fairing algorithm in reducing the MSE of gamma estimates for appropriately chosen damping factor τ. This ratio of the MSEs seems to be minimized when τ is in a neighborhood of 0.5, which coincides with our choice of $\tau = 0.5$ in the previous sections.

5.2. *Dependent case*

Now, let us look at two examples to illustrate how payoff functions affect the resulting correlation structure of the estimates p_i and thus that of the Z_i. The first example is when the payoff function is $\mathbf{1}_{\{S(x)\ge 0.5\}}$ and $S(x) = xU$, where U is a uniform random variable with values in [0, 1]. Thus,

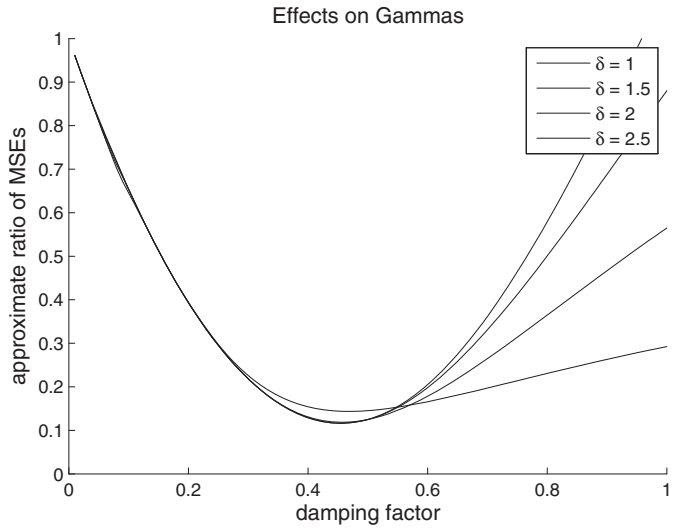

Fig. 9. The effects of δ and τ on the ratio of MSEs for $\Gamma_{i,1}$ and $\widehat{\Gamma}_i$.

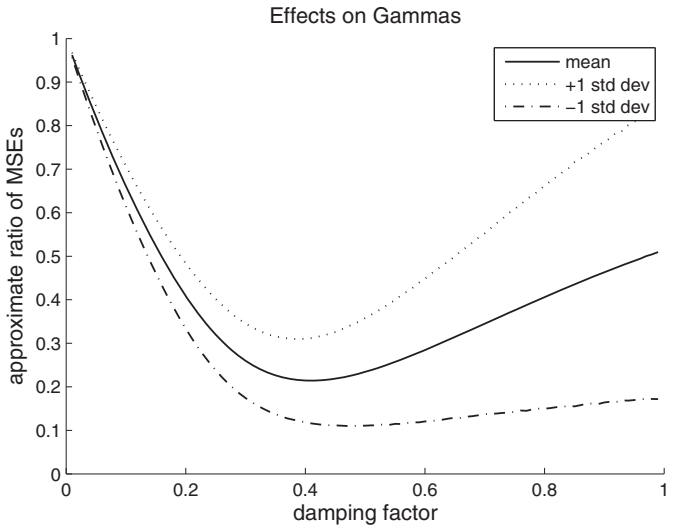

Fig. 10. The effects of τ on the ratio of MSEs, using 1000 randomly generated correlation structures.

the true price (or expected payoff) is $\alpha(x) = (1 - 1/(2x))^+$ and the corresponding Monte Carlo estimates are given by

$$p_i = \frac{1}{m}\sum_{k=1}^{m} \mathbf{1}_{\{U_k \geq n/(2i)\}}, \quad i = 0, \ldots, n,$$

after m simulation trials where the U_k are independent and identically distributed uniform random variables. It is also easy to compute the variance and covariance of p_i. With $i < j$

$$\mathsf{Var}(p_i) = \frac{1}{m}\alpha_i(1-\alpha_i) = \frac{(2i/n-1)^+}{4i^2m/n^2},$$
$$\mathsf{Cov}(p_i, p_j) = \frac{1}{m}\alpha_i(1-\alpha_j) = \frac{(2i/n-1)^+}{4ijm/n^2},$$

from which we notice that the correlation matters only when $i/n > 0.5$ and

$$\mathsf{Corr}(p_i, p_j) = \sqrt{\frac{2i-n}{2j-n}}.$$

For comparison, consider the second payoff function given by $S(x) = xU$ itself. Then, $\alpha(x) = x/2$ and the correlation is always one. Therefore, when the payoff function involves more exotic features with discontinuities, we expect that the correlation structure would exhibit more apparent departure from the perfect correlation case. This leads to greatly fluctuating discrete gamma estimates and consequently the common random number technique becomes non-satisfactory in producing stable gammas.

For the rest of this section, we investigate how the algorithm performs in the presence of non-trivial correlation structures. Let τ be fixed. For a given correlation structure, we generate correlated normal random vectors of length 7. Using those random vectors, we compute $E[(A_{i+1} - 2A_i + A_{i-1})^2]$ with and without fairing applied, where the expectations are set as the averages of 10^4 trials. Finally, the approximate ratio of MSEs is computed for this fixed τ and fixed correlation structure.

To see the average performance of the algorithm based on many different correlation structures, we used 1000 random instances of correlation structures. Then, for each fixed τ, the mean and standard deviation of approximate ratios of MSEs were obtained. Figure 10 shows those values for damping factor τ varying in [0, 1] together with ± 1 standard deviations. We observe a similar performance as in Fig. 9. There could be many different ways to produce various instances of correlation structures. One simple way we take here is to generate a 7×7 matrix such that entries are independent standard normals. If we divide each row by its magnitude and denote the resulting matrix by $\mathbf{F}$, then $\mathbf{Z} = \mathbf{FW}$ with $\mathbf{W}$ standard normal vector of size 7 becomes correlated normals.

Remark 2. So far, we have discussed the effectiveness of the fairing algorithm in terms of MSEs by focusing on the first iteration of the algorithm. Instead, we can also analyze the algorithm by looking at some specific examples. Figures 11 and 12 present the ratios of MSEs of faired estimates and the original FD estimates when we vary τ and δ, respectively. The contingent claim used is DO from Section 4, but we observe similar behaviors for other examples.

Even though the analysis of the first iteration shows that the optimal τ seems to be around 0.5, the MSE ratio flattens as the number of iterations increases, making the fairing result insensitive to τ as shown in Fig. 11. However, for small τ values, the algorithm requires a large number of iterations, slowing down the convergence. On the other hand, for the examples used in this article, we found that the

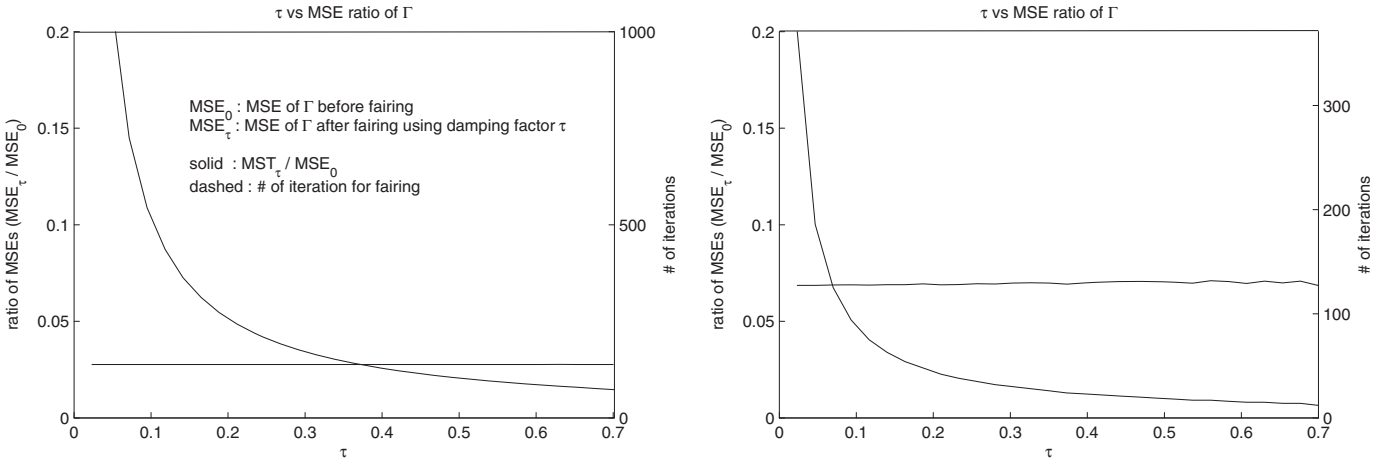

Fig. 11. The effects of τ on the ratio of MSEs for DO with $\delta = 1$: (left) 10^4 paths and (right) 10^6 paths.

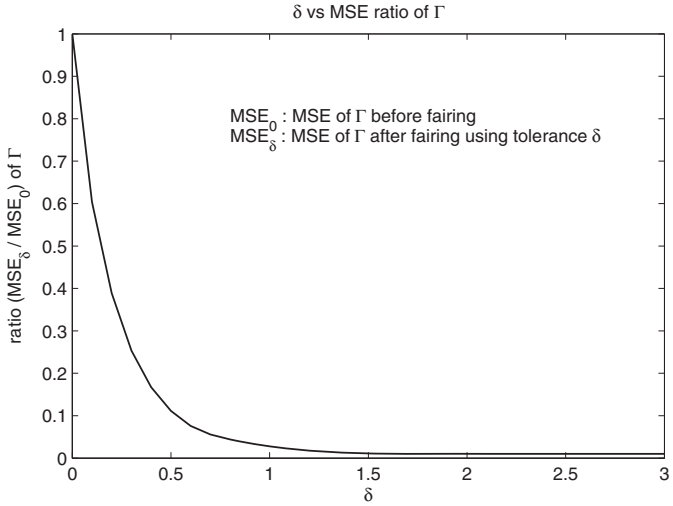

Fig. 12. The effects of δ on the ratio of MSEs for DO with $\tau = 0.5$.

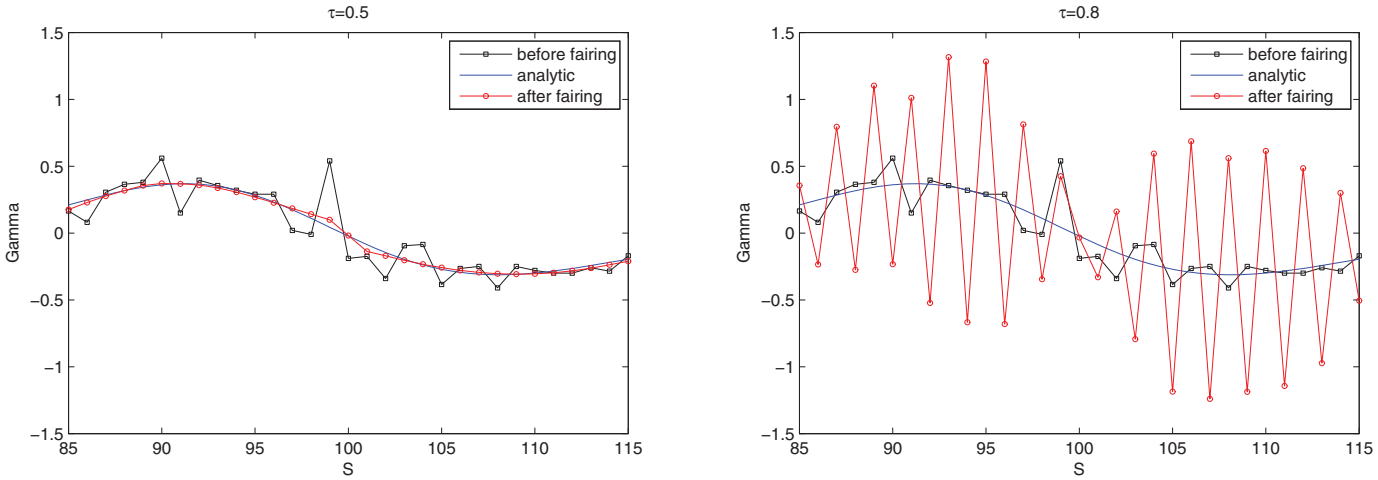

Fig. 13. Gamma curves for DO with $\delta = 1$: (left) $\tau = 0.5$ and (right) $\tau = 0.8$.

fairing algorithm may fail to converge for large τ values as in Fig. 13. (The algorithm converges for every $\tau < 0.75$ in all numerical tests conducted.) Therefore, $\tau = 0.5$ can be regarded as a reasonable choice that achieves convergence and efficiency.

Regarding fairing tolerance, the ratio of MSEs decreases as δ increases, as one can easily expect. However, we observe from curves of the MSE ratio that there is very little improvement by increasing δ when δ is greater than one. See Fig. 12 for an illustration of a typical case. On the other hand, it would not be desirable to alter final price estimates too much from the original Monte Carlo estimates. Hence, we suggest using δ between one and 1.5 as a practical choice for algorithm effectiveness; i.e., we change price estimates within one or a bit larger standard error range. Note that we used $\delta = 1$ for the numerical tests in Section 4.

6. Concluding remarks

Fairing is a collection of techniques that have been used in digital shape reconstruction. We introduced a simple curve/surface fairing algorithm to achieve reliable gamma estimates for complex financial derivatives. Instead of smoothing gamma curves or surfaces themselves, the algorithm varies the price estimates p_i within a small interval $[p_i - \delta\sigma, p_i + \delta\sigma]$ so that the new price estimates are still good candidates for the true prices. This small interval is determined by the fairing tolerance δ. Another important parameter in the algorithm is the damping factor τ, which controls the oscillation of estimates from one iteration to the next.

Pictorial and numerical examples are provided to demonstrate the performance of the method for complex exotic equity derivatives that are currently traded in Korean financial markets with great popularity. With no extra cost of applying the algorithm (as it is simple and fast), we observed that more stable gamma values are produced. Since Monte Carlo simulation is often the only method to rely on when it comes to the pricing and hedging of exotic derivatives, the importance of reliable and stable gamma values cannot be overemphasized.

Finally, we showed the performance of the fairing algorithm in terms of relative MSEs of the gamma estimates $\Gamma_{i,1}$ after the first iteration with respect to the gamma estimates $\widehat{\Gamma}_i$ without fairing. It is shown that it achieves more than on 80% decrease in the MSE with the damping factor $\tau \approx 0.5$. Also, through examples, we demonstrated that parameter values $\tau = 0.5$ and δ between one and 1.5 are a reasonable choice in implementing the algorithm.

Acknowledgements

Part of this project was completed while the second-named author was visiting the Fields Institute in Toronto, Canada. Their support and hospitality are greatly appreciated.

Funding

Kang's work was supported by the National Research Foundation of Korea (NRF) grant funded by the Korea government (MEST) (No. 2009-0068043). Kim's work was supported by the Basic Science Research Program through the NRF funded by the MEST (grant 2011-0007651). Shin's work was supported by DAPA and ADD (grant UD110006MD).

References

Broadie, M.N. and Glasserman, P. (1996) Estimating security price derivatives using simulation. *Management Science*, **42**, 269–285.

Cho, S. and Choi, B. (2001) Analysis of difference fairing based on DFT filter. *Computer-Aided Design*, **33**, 45–56.

Eck, M. and Jaspert, R. (1994) Automatic fairing of point sets, in *Designing Fair Curves and Surfaces*, Sapidis, N. (ed), SIAM, Philadelphia, PA, pp. 45–60.

Fournié, E., Lasry, J.-M., Lebuchoux, J. and Lions, P.-L. (2001) Applications of Malliavin calculus to Monte Carlo methods in finance II. *Finance and Stochastics*, **5**, 201–236.

Fournié, E., Lasry, J.-M., Lebuchoux, J., Lions, P.-L. and Touzi, N. (1999) Applications of Malliavin calculus to Monte Carlo methods in finance. *Finance and Stochastics*, **3**, 391–412.

Giles, M.B. and Glasserman, P. (2006). Smoking adjoints: fast Monte Carlo Greeks. *Risk*, **19**, 88–92.

Glasserman, P. (2004). *Monte Carlo Methods in Financial Engineering*, Springer, New York, NY.

Kang, W., Kim, K. and Shin, H. (2012) Denoising Monte Carlo sensitivity estimates. *Operations Research Letters*, **40**, 195–202.

Salvi, P. and Várady, T. (2005) Local fairing of freeform curves and surfaces, in *Proceedings of the Third Hungarian Conference on Computer Graphics and Geometry*, pp. 1493–1501.

Sapidis, N. and Farin, G. (1990) Automatic fairing algorithm for B-spline curves. *Computer-Aided Design*, **22**, 121–129.

Sun, X., Rosin, P.L., Martin, R.R. and Langbein, F.C. (2008) Random walks for feature-preserving mesh denoising. *Computer Aided Geometric Design*, **25**, 437–456.

Taleb, N. (1997) *Dynamic Hedging: Managing Vanilla and Exotic Options*, Wiley, New York, NY.

Yamada, A., Shimada, K., Furuhata, T. and Hou, K.-H. (1999) A discrete spring model for generating fair curves and surfaces, in *Proceedings of the Seventh Pacific Conference on Computer Graphics and Applications*, pp. 270–279.

Zhang, C., Zhang, P. and Cheng, F. (2001) Fairing spline curves and surface by minimizing energy. *Computer-Aided Design*, **33**, 913–923.

Appendix A: Numerical results

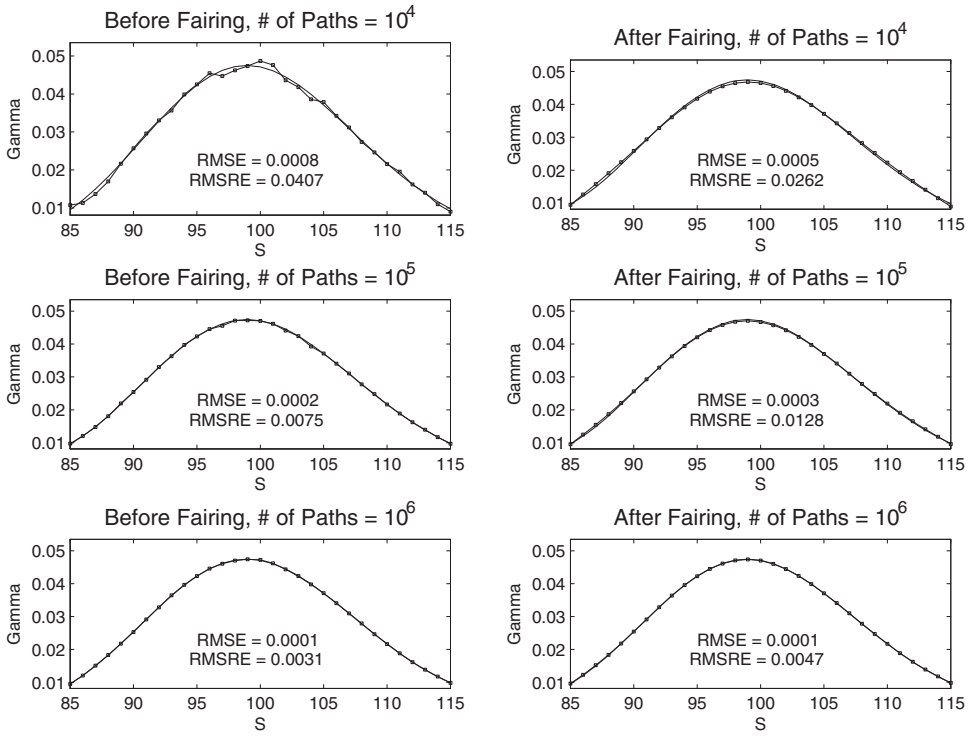

Fig. A1. Gamma curves for CO.

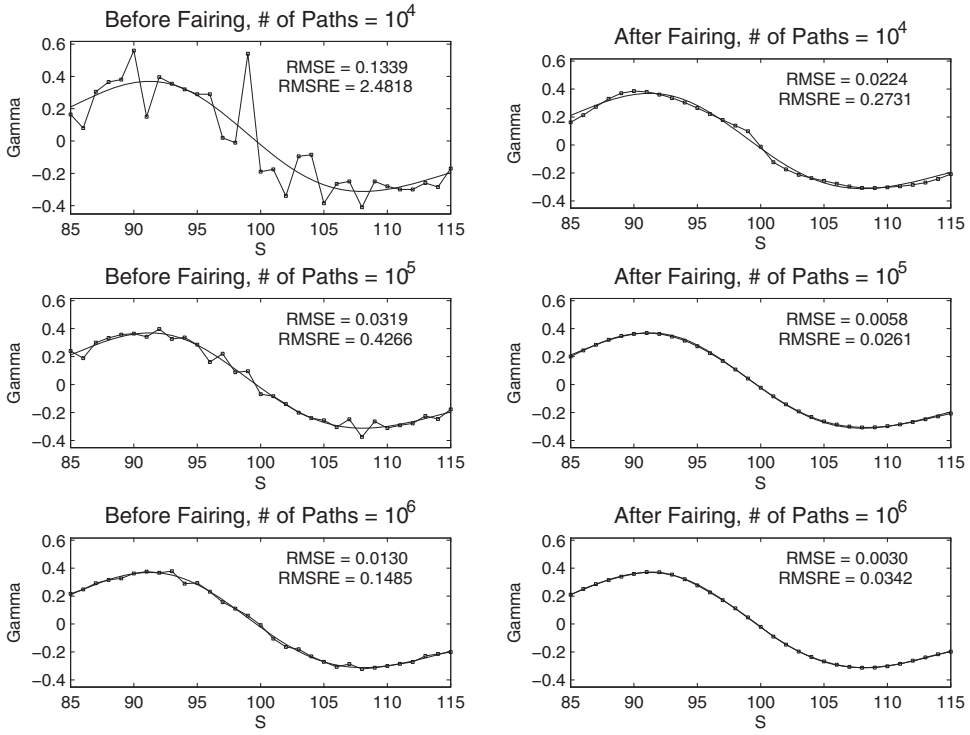

Fig. A2. Gamma curves for DO.

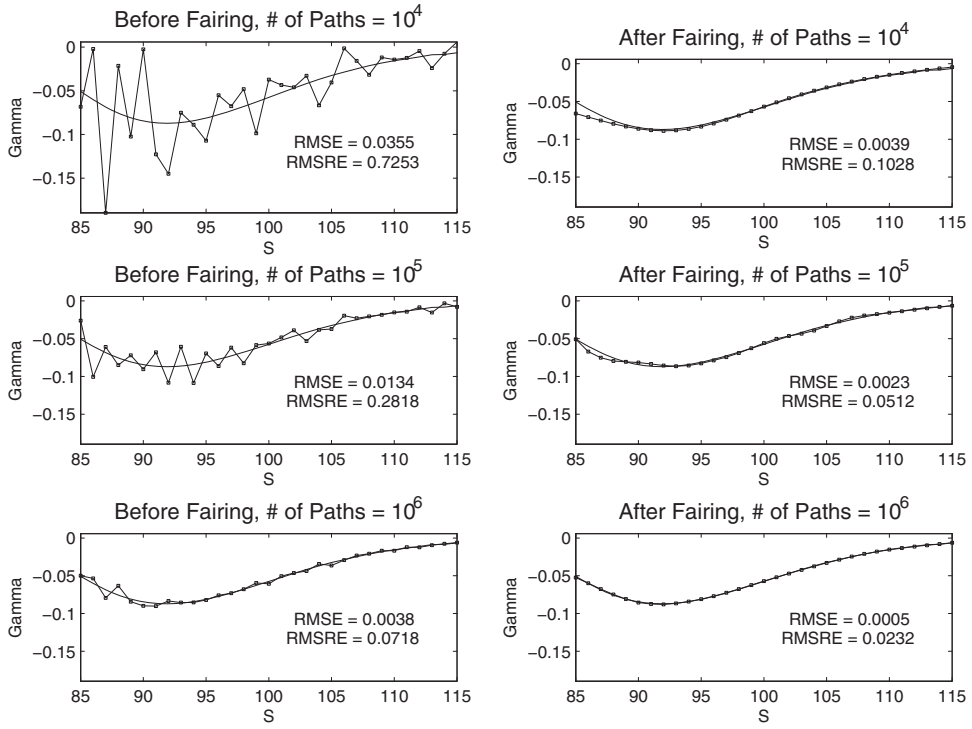

Fig. A3. Gamma curves for ELS1.

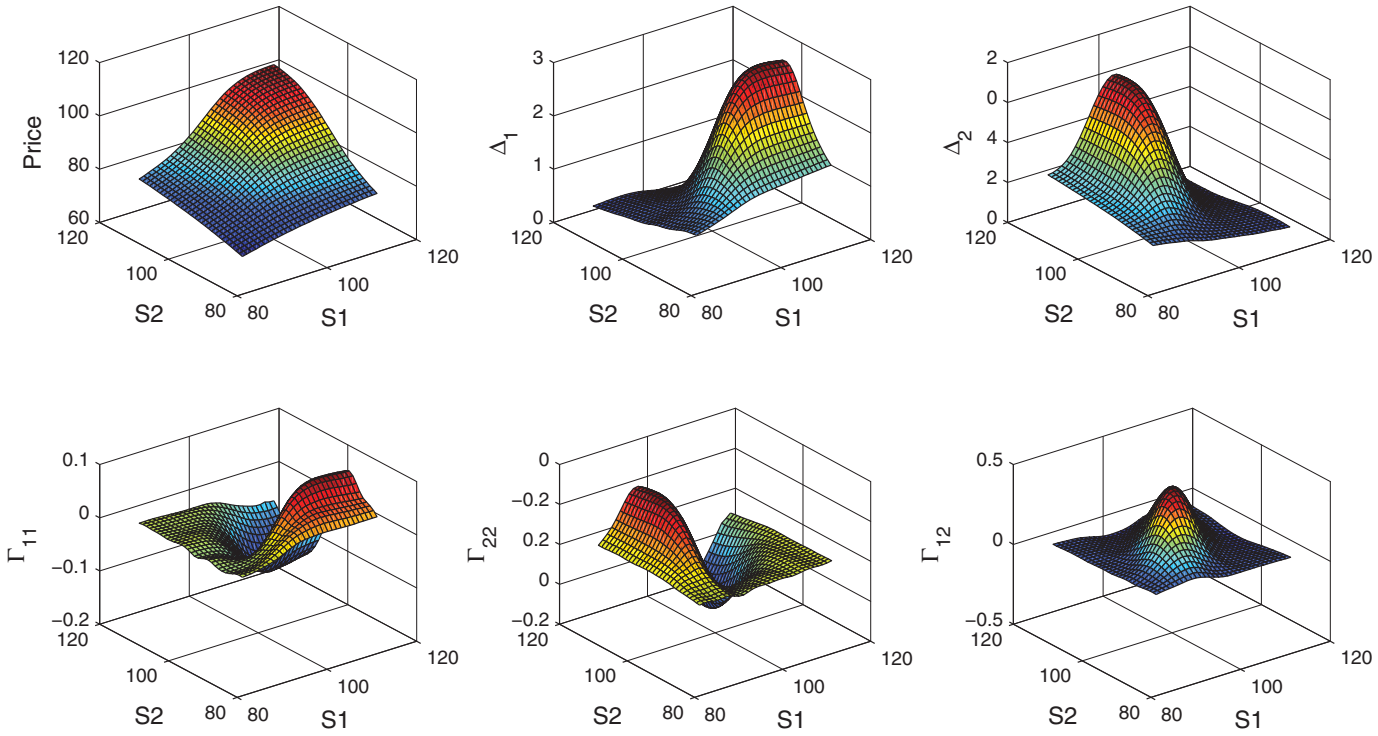

Fig. A4. Price, delta, gamma surfaces for ELS2 after fairing.

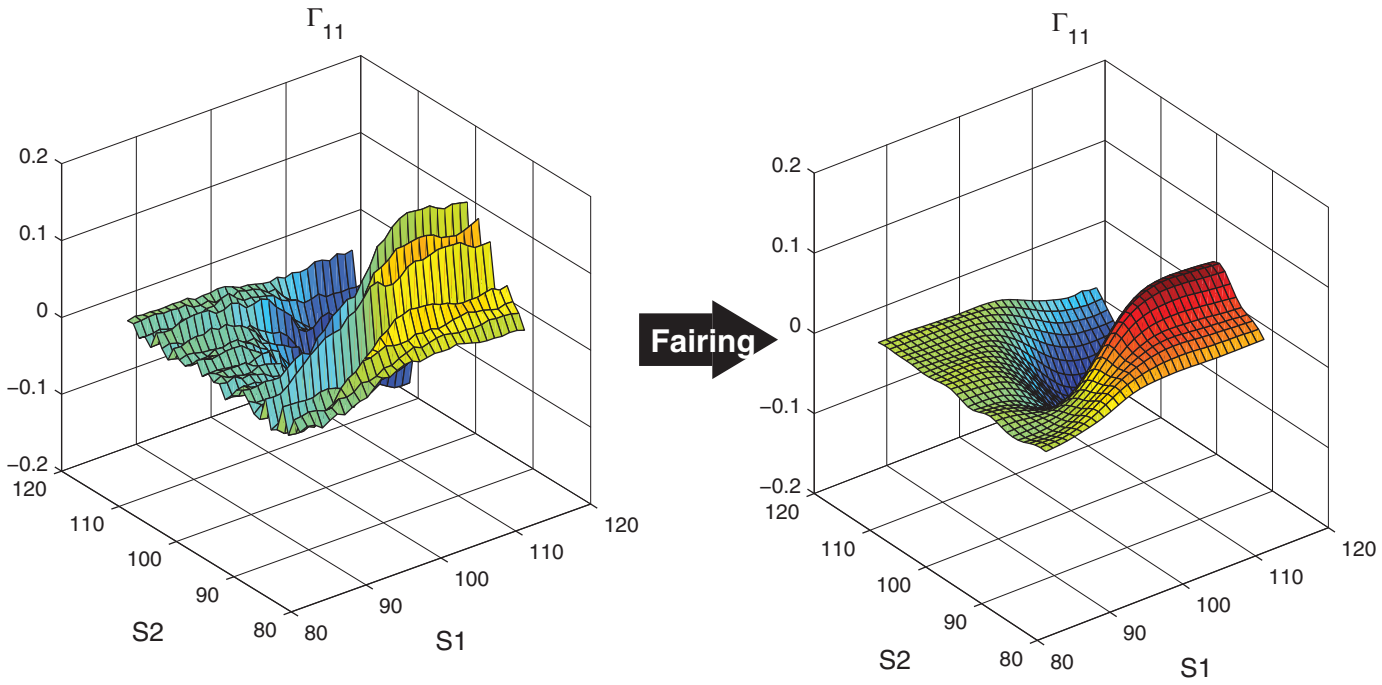

Fig. A5. Changes of Γ_{11} surfaces for ELS2.

Table A1. Fairing performance for CO, number of sample paths = 10^4

		RMSE		*Ratio*	*RMSRE (%)*		*Ratio*
	Volatility	*None*	*Fairing*	*Fairing/none*	*None*	*Fairing*	*Fairing/none*
Price	0.1	0.008 431	0.010 312	1.223	6.056 399	3.440 069	0.568
	0.2	0.009 865	0.011 016	1.117	6.495 915	2.188 127	0.337
	0.3	0.004 483	0.011 717	2.614	0.754 664	1.288 579	1.707
	0.4	0.043 476	0.030 359	0.698	2.532 658	2.064 095	0.815
	0.5	0.019 260	0.039 004	2.025	1.286 652	1.877 689	1.459
Delta	0.1	0.001 725	0.002 754	1.596	6.227 193	4.892 254	0.786
	0.2	0.001 146	0.001 505	1.313	5.744 987	2.004 467	0.349
	0.3	0.000 861	0.001 845	2.142	1.863 818	1.034 105	0.555
	0.4	0.001 667	0.001 906	1.143	0.708 596	0.548 860	0.775
	0.5	0.002 209	0.002 030	0.919	0.603 340	0.744 392	1.234
Gamma	0.1	0.001 304	0.001 431	1.097	31.206 356	43.310 057	1.388
	0.2	0.000 818	0.000 498	0.609	4.687 777	2.877 317	0.614
	0.3	0.000 809	0.000 509	0.629	4.073 068	2.623 079	0.644
	0.4	0.000 790	0.000 504	0.639	3.101 856	2.255 516	0.727
	0.5	0.001 006	0.000 421	0.419	4.345 946	1.778 993	0.409

Table A2. Fairing performance for CO, number of sample paths = 10^5

		RMSE		*Ratio*	*RMSRE (%)*		*Ratio*
	Volatility	*None*	*Fairing*	*Fairing/none*	*None*	*Fairing*	*Fairing/none*
Price	0.1	0.000 625	0.000 499	0.799	1.198 545	2.165 792	1.807
	0.2	0.001 281	0.001 031	0.804	1.528 602	0.540 757	0.354
	0.3	0.012 215	0.014 139	1.158	1.558 366	1.243 107	0.798
	0.4	0.011 412	0.007 892	0.692	0.720 879	0.573 542	0.796
	0.5	0.002 801	0.006 546	2.337	0.074 107	0.279 549	3.772
Delta	0.1	0.000 367	0.000 238	0.648	2.593 194	4.000 983	1.543
	0.2	0.000 433	0.000 394	0.910	0.590 155	0.978 936	1.659
	0.3	0.000 717	0.001 187	1.655	0.819 275	0.701 442	0.856
	0.4	0.000 566	0.000 686	1.212	0.242 859	0.256 121	1.055
	0.5	0.000 423	0.000 821	1.941	0.118 531	0.320 519	2.704
Gamma	0.1	0.000 431	0.000 401	0.931	9.481 634	22.353 851	2.358
	0.2	0.000 366	0.000 241	0.657	1.928 106	0.932 435	0.484
	0.3	0.000 208	0.000 269	1.295	0.746 287	1.275 929	1.710
	0.4	0.000 294	0.000 207	0.706	1.135 561	0.977 121	0.860
	0.5	0.000 196	0.000 184	0.938	0.874 006	0.817 375	0.935

Table A3. Fairing performance for CO, number of sample paths = 10^6

		RMSE		*Ratio*	*RMSRE (%)*		*Ratio*
	Volatility	*None*	*Fairing*	*Fairing/none*	*None*	*Fairing*	*Fairing/none*
Price	0.1	0.000 275	0.000 184	0.669	0.121 964	0.431 934	3.541
	0.2	0.000 511	0.000 918	1.797	0.685 632	1.197 275	1.746
	0.3	0.001 030	0.001 618	1.571	0.103 982	0.108 245	1.041
	0.4	0.001 802	0.001 087	0.603	0.050 889	0.062 015	1.219
	0.5	0.005 781	0.007 900	1.366	0.189 364	0.273 682	1.445
Delta	0.1	0.000 097	0.000 103	1.058	0.249 694	0.639 947	2.563
	0.2	0.000 138	0.000 244	1.773	0.507 179	0.939 763	1.853
	0.3	0.000 103	0.000 226	2.197	0.068 867	0.189 072	2.745
	0.4	0.000 250	0.000 211	0.846	0.070 394	0.073 581	1.045
	0.5	0.000 187	0.000 415	2.220	0.069 341	0.189 217	2.729
Gamma	0.1	0.000 076	0.000 214	2.822	3.434 934	8.077 912	2.352
	0.2	0.000 107	0.000 096	0.900	0.696 168	0.543 899	0.781
	0.3	0.000 082	0.000 074	0.902	0.313 318	0.468 134	1.494
	0.4	0.000 086	0.000 070	0.812	0.325 209	0.301 834	0.928
	0.5	0.000 118	0.000 064	0.543	0.525 378	0.298 024	0.567

Table A4. Fairing performance for DO, number of sample paths = 10^4

		RMSE		*Ratio*	*RMSRE (%)*		*Ratio*
	Volatility	*None*	*Fairing*	*Fairing/none*	*None*	*Fairing*	*Fairing/none*
Price	0.1	0.177 991	0.204 037	1.146	6.204 482	7.161 622	1.154
	0.2	0.144 163	0.155 648	1.080	5.732 985	4.669 140	0.814
	0.3	0.093 758	0.059 618	0.636	1.999 274	1.495 868	0.748
	0.4	0.168 825	0.097 084	0.575	0.595 954	0.237 579	0.399
	0.5	0.227 867	0.176 645	0.775	0.719 249	0.610 910	0.849
Delta	0.1	0.091 601	0.085 297	0.931	21.590 139	24.636 857	1.141
	0.2	0.075 925	0.052 138	0.687	4.473 775	1.926 412	0.431
	0.3	0.068 504	0.029 330	0.428	3.308 067	1.777 163	0.537
	0.4	0.066 104	0.023 914	0.362	2.232 643	1.232 896	0.552
	0.5	0.078 895	0.033 109	0.420	3.397 535	1.621 266	0.477
Gamma	0.1	0.184 289	0.070 915	0.385	136.011 529	59.310 041	0.436
	0.2	0.197 668	0.026 891	0.136	83.801 240	6.686 550	0.080
	0.3	0.133 909	0.022 409	0.167	248.176 466	27.313 975	0.110
	0.4	0.196 291	0.012 310	0.063	667.814 406	16.996 175	0.025
	0.5	0.145 305	0.010 608	0.073	23289.509 582	212.832 827	0.009

Table A5. Fairing performance for DO, number of sample paths = 10^5

		RMSE		*Ratio*	*RMSRE (%)*		*Ratio*
	Volatility	*None*	*Fairing*	*Fairing/none*	*None*	*Fairing*	*Fairing/none*
Price	0.1	0.048 711	0.031 598	0.649	2.839 865	4.757 498	1.675
	0.2	0.051 435	0.045 635	0.887	0.359 608	0.874 123	2.431
	0.3	0.066 943	0.099 913	1.493	0.747 506	0.992 980	1.328
	0.4	0.058 959	0.037 956	0.644	0.268 482	0.174 729	0.651
	0.5	0.041 649	0.029 571	0.710	0.135 095	0.074 141	0.549
Delta	0.1	0.038 277	0.026 569	0.694	8.542 883	13.584 750	1.590
	0.2	0.032 428	0.025 313	0.781	1.414 315	1.802 560	1.275
	0.3	0.014 477	0.017 056	1.178	0.594 527	0.573 660	0.965
	0.4	0.026 170	0.016 340	0.624	1.020 187	0.747 576	0.733
	0.5	0.015 758	0.006 374	0.404	0.692 426	0.244 048	0.352
Gamma	0.1	0.085 309	0.063 838	0.748	21.708 945	19.606 209	0.903
	0.2	0.042 971	0.017 349	0.404	24.398 032	4.846 873	0.199
	0.3	0.031 946	0.005 791	0.181	42.658 058	2.606 274	0.061
	0.4	0.047 244	0.006 809	0.144	76.938 641	14.543 675	0.189
	0.5	0.040 049	0.002 171	0.054	155.816 662	166.204 966	1.067

Table A6. Fairing performance for DO, number of sample paths = 10^6

		RMSE		*Ratio*	*RMSRE (%)*		*Ratio*
	Volatility	*None*	*Fairing*	*Fairing/none*	*None*	*Fairing*	*Fairing/none*
Price	0.1	0.009 760	0.006 458	0.662	0.333 251	0.881 242	2.644
	0.2	0.014 863	0.022 572	1.519	0.511 282	0.896 094	1.753
	0.3	0.009 818	0.011 665	1.188	0.055 361	0.100 499	1.815
	0.4	0.025 664	0.019 397	0.756	0.078 652	0.052 960	0.673
	0.5	0.018 673	0.017 536	0.939	0.071 071	0.074 206	1.044
Delta	0.1	0.006 364	0.005 007	0.787	2.887 798	2.893 965	1.002
	0.2	0.007 903	0.007 984	1.010	0.406 854	0.579 385	1.424
	0.3	0.006 528	0.003 615	0.554	0.258 660	0.144 399	0.558
	0.4	0.007 930	0.005 385	0.679	0.291 070	0.174 859	0.601
	0.5	0.010 076	0.004 172	0.414	0.460 961	0.209 221	0.454
Gamma	0.1	0.010 948	0.012 300	1.123	10.685 524	9.064 668	0.848
	0.2	0.014 575	0.005 231	0.359	9.889 703	1.933 308	0.195
	0.3	0.012 971	0.003 025	0.233	14.849 271	3.415 856	0.230
	0.4	0.018 651	0.002 106	0.113	52.548 515	5.453 844	0.104
	0.5	0.013 359	0.002 584	0.193	661.434 011	150.584 595	0.228

Table A7. Fairing performance for ELS1, number of sample paths = 10^4

		RMSE		*Ratio*	*RMSRE (%)*		*Ratio*
	Maturity	*None*	*Fairing*	*Fairing/none*	*None*	*Fairing*	*Fairing/none*
Price	1M	0.026 772	0.015 176	0.567	0.024 156	0.013 683	0.566
	3M	0.043 370	0.035 100	0.809	0.040 728	0.032 964	0.809
	5M	0.091 541	0.116 871	1.277	0.090 537	0.116 250	1.284
	7M	0.060 849	0.087 711	1.441	0.063 189	0.092 160	1.458
	9M	0.124 374	0.154 804	1.245	0.131 593	0.164 284	1.248
	11M	0.106 448	0.111 599	1.048	0.113 904	0.120 635	1.059
Delta	1M	0.008 870	0.004 243	0.478	45.042 267	29.009 132	0.644
	3M	0.013 627	0.007 820	0.574	11.125 575	2.836 769	0.255
	5M	0.018 166	0.010 850	0.597	3.791 569	5.074 421	1.338
	7M	0.026 126	0.009 932	0.380	6.885 227	3.272 720	0.475
	9M	0.025 667	0.014 513	0.565	5.461 150	3.087 952	0.565
	11M	0.027 759	0.011 158	0.402	6.378 829	2.920 302	0.458
Gamma	1M	0.013 089	0.001 605	0.123	170.944 067	61.484 846	0.360
	3M	0.030 933	0.004 728	0.153	94.916 265	7.814 702	0.082
	5M	0.036 285	0.002 407	0.066	83.672 159	8.892 477	0.106
	7M	0.042 971	0.003 351	0.078	119.386 012	10.844 639	0.091
	9M	0.043 630	0.004 873	0.112	142.049 137	19.154 051	0.135
	11M	0.039 148	0.004 551	0.116	158.717 747	22.222 170	0.140

Table A8. Fairing performance for ELS1, number of sample paths = 10^5

		RMSE		*Ratio*	*RMSRE (%)*		*Ratio*
	Maturity	*None*	*Fairing*	*Fairing/none*	*None*	*Fairing*	*Fairing/none*
Price	1M	0.009 988	0.009 041	0.905	0.009 172	0.008 248	0.899
	3M	0.015 732	0.012 036	0.765	0.015 271	0.011 556	0.757
	5M	0.028 741	0.023 026	0.801	0.028 781	0.023 004	0.799
	7M	0.023 301	0.018 377	0.789	0.023 292	0.018 151	0.779
	9M	0.026 116	0.017 394	0.666	0.026 662	0.017 613	0.661
	11M	0.034 854	0.028 540	0.819	0.036 485	0.029 925	0.820
Delta	1M	0.003 476	0.001 551	0.446	25.007 081	26.501 342	1.060
	3M	0.005 888	0.003 144	0.534	3.023 069	2.804 295	0.928
	5M	0.007 681	0.002 870	0.374	3.397 839	2.278 815	0.671
	7M	0.007 702	0.001 995	0.259	2.768 374	1.624 420	0.587
	9M	0.006 119	0.001 078	0.176	1.544 639	0.551 511	0.357
	11M	0.006 672	0.001 437	0.215	1.788 126	0.802 062	0.449
Gamma	1M	0.006 361	0.001 189	0.187	77.965 766	68.387 683	0.877
	3M	0.010 540	0.001 209	0.115	37.974 661	4.815 578	0.127
	5M	0.011 789	0.000 906	0.077	35.792 781	3.783 252	0.106
	7M	0.014 614	0.000 600	0.041	40.307 293	3.452 645	0.086
	9M	0.010 928	0.000 322	0.029	37.409 181	1.460 261	0.039
	11M	0.014 552	0.000 454	0.031	64.440 685	2.231 438	0.035

Table A9. Fairing performance for ELS1, number of sample paths = 10^6

		RMSE		*Ratio*	*RMSRE (%)*		*Ratio*
	Maturity	*None*	*Fairing*	*Fairing/none*	*None*	*Fairing*	*Fairing/none*
Price	1M	0.002 658	0.003 407	1.282	0.002 420	0.003 102	1.282
	3M	0.004 025	0.003 688	0.916	0.003 808	0.003 525	0.926
	5M	0.004 892	0.005 633	1.151	0.004 695	0.005 434	1.157
	7M	0.005 648	0.004 725	0.837	0.005 663	0.004 631	0.818
	9M	0.003 963	0.004 648	1.173	0.004 114	0.004 826	1.173
	11M	0.003 954	0.005 322	1.346	0.004 195	0.005 490	1.309
Delta	1M	0.000 981	0.000 581	0.593	29.978 766	27.903 137	0.931
	3M	0.001 475	0.001 174	0.796	1.235 948	0.779 192	0.630
	5M	0.001 713	0.000 904	0.528	0.832 191	0.692 663	0.832
	7M	0.002 042	0.001 163	0.570	0.810 540	0.808 872	0.998
	9M	0.002 009	0.000 596	0.297	0.684 755	0.275 490	0.402
	11M	0.001 970	0.000 744	0.377	0.642 783	0.309 150	0.481
Gamma	1M	0.001 526	0.000 708	0.464	69.692 625	52.667 074	0.756
	3M	0.003 849	0.000 497	0.129	11.540 481	4.395 740	0.381
	5M	0.003 209	0.000 273	0.085	8.402 842	1.490 872	0.177
	7M	0.003 910	0.000 388	0.099	11.863 576	1.949 523	0.164
	9M	0.004 715	0.000 269	0.057	15.575 413	1.062 526	0.068
	11M	0.004 420	0.000 167	0.038	17.578 385	0.780 319	0.044

Table A10. Fairing performance for ELS2, number of sample paths = 10^4

		RMSE		*Ratio*	*RMSRE (%)*		*Ratio*
	Maturity	*None*	*Fairing*	*Fairing/none*	*None*	*Fairing*	*Fairing/none*
Price	1M	0.033 084	0.026 732	0.808	0.029 835	0.024 098	0.808
	3M	0.057 145	0.059 545	1.042	0.054 356	0.056 950	1.048
	5M	0.130 751	0.140 888	1.078	0.131 126	0.141 777	1.081
	7M	0.082 856	0.092 738	1.119	0.088 028	0.098 868	1.123
	9M	0.131 875	0.150 059	1.138	0.141 872	0.162 125	1.143
	11M	0.108 610	0.109 098	1.004	0.118 138	0.119 415	1.011
Delta 1	1M	0.008 793	0.006 660	0.757	59.427 882	42.770 070	0.720
	3M	0.012 892	0.006 206	0.481	10.095 031	4.211 589	0.417
	5M	0.017 210	0.006 946	0.404	6.033 619	2.280 254	0.378
	7M	0.021 428	0.009 625	0.449	6.950 013	3.524 935	0.507
	9M	0.022 969	0.011 262	0.490	6.221 762	3.063 781	0.492
	11M	0.024 212	0.010 417	0.430	6.621 264	3.728 343	0.563
Delta 2	1M	0.005 573	0.002 251	0.404	453.964 648	409.756 625	0.903
	3M	0.013 558	0.008 629	0.636	35.546 945	19.091 001	0.537
	5M	0.013 138	0.010 743	0.818	16.355 078	10.186 645	0.623
	7M	0.019 124	0.011 733	0.614	11.406 066	8.654 134	0.759
	9M	0.012 211	0.006 995	0.573	8.956 580	6.393 383	0.714
	11M	0.019 139	0.010 155	0.531	9.777 811	6.217 412	0.636
Gamma 11	1M	0.012 409	0.002 848	0.230	2042.119 060	338.539 397	0.166
	3M	0.030 306	0.004 581	0.151	117.069 119	14.322 664	0.122
	5M	0.033 010	0.001 925	0.058	111.551 933	6.343 803	0.057
	7M	0.035 884	0.003 199	0.089	128.218 000	13.422 504	0.105
	9M	0.040 377	0.003 873	0.096	156.904 086	15.582 539	0.099
	11M	0.035 805	0.005 519	0.154	166.655 311	28.578 097	0.171
Gamma 22	1M	0.009 358	0.001 493	0.160	1070.117 668	478.007 650	0.447
	3M	0.031 598	0.005 422	0.172	593.728 970	86.114 763	0.145
	5M	0.025 977	0.003 748	0.144	149.792 054	29.734 086	0.199
	7M	0.037 298	0.008 772	0.235	129.832 723	26.034 627	0.201
	9M	0.032 570	0.003 434	0.105	145.192 843	14.843 527	0.102
	11M	0.035 285	0.004 192	0.119	175.920 220	22.410 546	0.127
Gamma 12	1M	0.000 523	0.000 305	0.582	4046.771 682	1923.908 560	0.475
	3M	0.002 116	0.000 535	0.253	5106.211 309	1395.730 774	0.273
	5M	0.002 964	0.000 547	0.184	3091.679 720	515.772 550	0.167
	7M	0.003 465	0.000 965	0.278	3302.801 124	389.754 606	0.118
	9M	0.003 291	0.000 711	0.216	977.581 637	298.692 771	0.306
	11M	0.003 568	0.001 188	0.333	1009.590 933	905.007 315	0.896

Table A11. Fairing performance for ELS2, number of sample paths = 10^5

		RMSE		*Ratio*	*RMSRE (%)*		*Ratio*
	Maturity	*None*	*Fairing*	*Fairing/none*	*None*	*Fairing*	*Fairing/none*
Price	1M	0.009 949	0.008 403	0.845	0.009 134	0.007 698	0.843
	3M	0.016 027	0.013 773	0.859	0.015 579	0.013 329	0.856
	5M	0.026 624	0.024 659	0.926	0.026 776	0.024 846	0.928
	7M	0.019 818	0.018 349	0.926	0.020 201	0.018 702	0.926
	9M	0.021 299	0.017 138	0.805	0.022 602	0.017 972	0.795
	11M	0.029 558	0.026 948	0.912	0.032 072	0.029 229	0.911
Delta 1	1M	0.003 495	0.001 772	0.507	31.377 765	26.813 794	0.855
	3M	0.005 577	0.003 095	0.555	3.070 638	2.154 082	0.702
	5M	0.006 993	0.003 174	0.454	3.189 354	1.516 771	0.476
	7M	0.006 380	0.002 032	0.319	2.445 714	1.044 479	0.427
	9M	0.006 041	0.002 043	0.338	1.754 497	0.654 452	0.373
	11M	0.005 968	0.002 216	0.371	1.724 396	0.803 891	0.466
Delta 2	1M	0.001 233	0.000 573	0.465	278.992 852	180.654 766	0.648
	3M	0.002 786	0.001 759	0.631	14.675 797	9.898 480	0.674
	5M	0.004 393	0.002 458	0.560	6.467 751	3.897 348	0.603
	7M	0.004 874	0.003 427	0.703	3.801 238	2.649 542	0.697
	9M	0.004 672	0.002 375	0.508	3.784 935	2.126 802	0.562
	11M	0.004 564	0.002 850	0.624	3.612 032	2.288 814	0.634
Gamma 11	1M	0.006 239	0.001 082	0.173	547.459 024	214.146 369	0.391
	3M	0.010 013	0.001 414	0.141	38.291 820	6.622 703	0.173
	5M	0.011 197	0.001 236	0.110	43.173 254	5.720 355	0.132
	7M	0.012 261	0.000 880	0.072	42.045 901	4.588 565	0.109
	9M	0.010 620	0.000 696	0.066	42.605 912	3.431 557	0.081
	11M	0.013 112	0.000 756	0.058	62.077 639	4.599 280	0.074
Gamma 22	1M	0.001 819	0.000 712	0.391	511.204 917	205.932 286	0.403
	3M	0.006 808	0.001 286	0.189	315.426 466	111.532 618	0.354
	5M	0.009 748	0.000 922	0.095	53.359 035	9.989 504	0.187
	7M	0.011 297	0.001 035	0.092	46.575 628	8.202 007	0.176
	9M	0.009 781	0.000 918	0.094	41.572 930	7.708 663	0.185
	11M	0.010 467	0.000 896	0.086	51.193 592	7.626 556	0.149
Gamma 12	1M	0.000 176	0.000 142	0.810	2443.485 241	1800.273 969	0.737
	3M	0.000 636	0.000 179	0.281	1326.216 089	520.126 928	0.392
	5M	0.000 926	0.000 292	0.315	720.166 137	531.307 996	0.738
	7M	0.001 036	0.000 290	0.280	956.262 255	250.915 086	0.262
	9M	0.001 030	0.000 265	0.258	443.069 192	88.899 924	0.201
	11M	0.001 071	0.000 325	0.304	693.343 928	198.121 479	0.286

Table A12. Fairing performance for ELS2, number of sample paths = 10^6

		RMSE		*Ratio*	*RMSRE (%)*		*Ratio*
	Maturity	*None*	*Fairing*	*Fairing/none*	*None*	*Fairing*	*Fairing/none*
Price	1M	0.002 911	0.003 525	1.211	0.002 651	0.003 209	1.211
	3M	0.006 726	0.005 754	0.856	0.006 346	0.005 449	0.859
	5M	0.008 274	0.008 704	1.052	0.008 114	0.008 606	1.061
	7M	0.006 961	0.007 053	1.013	0.007 018	0.007 093	1.011
	9M	0.007 541	0.007 990	1.060	0.008 049	0.008 484	1.054
	11M	0.009 645	0.010 000	1.037	0.010 537	0.010 814	1.026
Delta 1	1M	0.000 965	0.000 643	0.666	39.251 085	39.555 403	1.008
	3M	0.001 274	0.001 021	0.802	1.158 340	0.702 197	0.606
	5M	0.001 666	0.000 919	0.552	0.782 159	0.436 444	0.558
	7M	0.001 833	0.001 115	0.608	0.758 948	0.445 795	0.587
	9M	0.001 582	0.000 780	0.493	0.572 684	0.238 785	0.417
	11M	0.001 854	0.001 047	0.565	0.567 359	0.301 094	0.531
Delta 2	1M	0.000 420	0.000 511	1.218	148.585 265	137.128 162	0.923
	3M	0.001 024	0.000 776	0.757	5.628 705	4.719 485	0.838
	5M	0.001 665	0.000 938	0.563	1.518 567	1.410 389	0.929
	7M	0.001 657	0.001 002	0.605	1.104 430	0.640 570	0.580
	9M	0.001 802	0.000 993	0.551	1.029 175	0.564 742	0.549
	11M	0.001 682	0.000 816	0.485	0.893 341	0.561 947	0.629
Gamma 11	1M	0.001 493	0.000 712	0.477	216.048 600	205.834 303	0.953
	3M	0.003 803	0.000 481	0.126	14.561 589	4.020 437	0.276
	5M	0.003 293	0.000 354	0.108	10.747 362	1.881 142	0.175
	7M	0.003 645	0.000 398	0.109	12.615 216	1.882 688	0.149
	9M	0.003 767	0.000 306	0.081	14.507 076	1.416 406	0.098
	11M	0.003 833	0.000 439	0.114	17.604 703	2.437 236	0.138
Gamma 22	1M	0.000 869	0.000 507	0.584	241.660 508	162.651 063	0.673
	3M	0.002 140	0.000 316	0.148	95.880 964	80.676 162	0.841
	5M	0.003 074	0.000 440	0.143	16.351 848	2.938 703	0.180
	7M	0.005 245	0.000 396	0.076	15.688 571	1.922 473	0.123
	9M	0.003 441	0.000 457	0.133	14.335 122	3.430 490	0.239
	11M	0.003 329	0.000 303	0.091	15.133 258	2.420 689	0.160
Gamma 12	1M	0.000 106	0.000 099	0.934	1857.373 371	1626.926 020	0.876
	3M	0.000 221	0.000 096	0.435	373.803 350	218.324 963	0.584
	5M	0.000 305	0.000 112	0.369	262.351 788	200.695 015	0.765
	7M	0.000 324	0.000 129	0.399	254.714 631	136.117 780	0.534
	9M	0.000 369	0.000 114	0.308	125.985 431	28.771 846	0.228
	11M	0.000 380	0.000 118	0.310	164.644 789	48.020 995	0.292

Appendix B: Proofs

Proof of Lemma 1. For notational convenience, we denote $\tilde{A}_{i+1} - 2\tilde{A}_i + \tilde{A}_{i-1}$, $Z_{i+1} - 2Z_i + Z_{i-1}$ by $F + \tilde{G}$ and F, respectively. We define G in a similar way so that $A_{i+1} - 2A_i + A_{i-1} = F + G$. Then, in a straightforward manner, we get

$$\begin{aligned} &E[(\tilde{A}_{i+1} - 2\tilde{A}_i + \tilde{A}_{i-1})^2 - (A_{i+1} - 2A_i + A_{i-1})^2] \\ &\quad = E[(F + \tilde{G})^2 - (F + G)^2] \\ &\quad = E[2(F + G)(\tilde{G} - G) + (\tilde{G} - G)^2]. \end{aligned}$$

On the other hand, for any real numbers a and b, we have $|g(a + b) - g(b)| \le |a| \wedge (\delta\sigma)$. This leads us to $|\tilde{G} - G| \le \zeta_i$. Also, from $|g(a)| \le \delta\sigma$, $|G| \le 4\delta\sigma$. Since $E[|F|] = E[|Z_{i+1} - 2Z_i + Z_{i-1}|] = \sqrt{6}\sigma\, E[|\mathbf{Z}|]$ for a standard normal random variable Z, we get

$$\begin{aligned} &E[(\tilde{A}_{i+1} - 2\tilde{A}_i + \tilde{A}_{i-1})^2 - (A_{i+1} - 2A_i + A_{i-1})^2] \\ &\quad \le E\big[(2\sqrt{6}\sigma|Z| + 8\delta\sigma)\zeta_i + \zeta_i^2\big]. \end{aligned}$$

As for $\mathsf{E}[(\Gamma_{i,1} - \Gamma_i)^2]$ when $i = 1, 2, n-2, n-1$, we note that:

$$\begin{aligned} E[(\Gamma_{i,1} - \Gamma_i)^2] &= \frac{1}{h^4} E[(F + \tilde{G})^2] \le \frac{1}{h^4} E[(|F| + |\tilde{G}|)^2] \\ &\le \frac{1}{h^4} E[(\sqrt{6}\sigma|Z| + 4\delta\sigma)^2]. \end{aligned}$$

Combining above two observations and $\mathsf{E}[|Z|] = \sqrt{2/\pi}$ gives the result. ■

Proof of Proposition 1. Let us fix i and compute $E[A_i^2]$, $E[A_{i+1}A_{i-1}]$, and $E[A_iA_{i-1}]$ separately. For the first one, we proceed as follows:

$$\begin{aligned}E\left[A_i^2\right] &= E[(Z_i + g(\tau\boldsymbol{\varphi}\times\mathbf{Z}_i))^2]\\ &= E\left[Z_i^2 + 2Z_i g(\tau\boldsymbol{\varphi}\times\mathbf{Z}_i) + g(\tau\boldsymbol{\varphi}\times\mathbf{Z}_i)^2\right]\\ &= \sigma^2 + 2\sigma\mathsf{E}\left[Xg(\tau|\varphi|\sigma Y)\right] + \mathsf{E}[g(\tau|\varphi|\sigma Y)^2]\end{aligned}$$

where $X=\sigma^{-1}Z_i$ and $Y=(\sigma|\varphi|)^{-1}\boldsymbol{\varphi}\times\mathbf{Z}_i$. Then, it is easy to see that X, Y are two standard normal random variables with the correlation $\rho_1=-1/|\boldsymbol{\varphi}|$. Since we can write $\rho_1 Y+\sqrt{1-\rho_1^2}Z$ in place of X for an independent standard normal Z, we are led to

$$E[A_i^2]=\sigma^2+2\sigma\rho_1 E\left[Yg(\tau|\varphi|\sigma Y)\right]+E\left[g(\tau|\varphi|\sigma Y)^2\right].$$

The second one can be computed in a similar fashion,

$$\begin{aligned}&E[A_{i+1}A_{i-1}]\\ &= E\left[(Z_{i+1}+g(\tau\boldsymbol{\varphi}\times Z_{i+1}))(Z_{i-1}+g(\tau\boldsymbol{\varphi}\times\mathbf{Z}_{i-1}))\right]\\ &= E[Z_{i+1}g(\tau\varphi\cdot\mathbf{Z}_{i-1})+Z_{i-1}g(\tau\boldsymbol{\varphi}\times\mathbf{Z}_{i+1})\\ &\quad + g(\tau\boldsymbol{\varphi}\times\mathbf{Z}_{i+1})g(\tau\boldsymbol{\varphi}\times\mathbf{Z}_{i-1})]\\ &= E\left[2\sigma Xg(\tau|\boldsymbol{\varphi}|\sigma Y)+g(\tau|\boldsymbol{\varphi}|\sigma Y)g(\tau|\boldsymbol{\varphi}|\sigma Y')\right],\end{aligned}$$

where X, Y, and Y' are standard normal random variables with correlations $\rho_2=\mathsf{Corr}(X,Y)=-1/(6|\varphi|)$ and $\rho_3=\mathsf{Corr}(Y,Y')=7/(9|\varphi|^2)$. Again, using $\rho_2 Y+\sqrt{1-\rho_2^2}Z$ instead of X, we get:

$$\begin{aligned}E[A_{i+1}A_{i-1}] &= 2\sigma\rho_2 E\left[Yg(\tau|\boldsymbol{\varphi}|\sigma Y)\right]\\ &\quad + E\left[g(\tau|\boldsymbol{\varphi}|\sigma Y)g(\tau|\boldsymbol{\varphi}|\sigma Y')\right].\end{aligned}$$

Likewise, we obtain:

$$\begin{aligned}&E[A_iA_{i-1}]\\ &= E\left[(Z_i+g(\tau\boldsymbol{\varphi}\times\mathbf{Z}_i))(Z_{i-1}+g(\tau\boldsymbol{\varphi}\times\mathbf{Z}_{i-1}))\right]\\ &= E[Z_ig(\tau\boldsymbol{\varphi}\times\mathbf{Z}_{i-1})+Z_{i-1}g(\tau\boldsymbol{\varphi}\times\mathbf{Z}_i)\\ &\quad + g(\tau\boldsymbol{\varphi}\times\mathbf{Z}_i)g(\tau\boldsymbol{\varphi}\times\mathbf{Z}_{i-1})]\\ &= E\left[2\sigma Xg(\tau|\boldsymbol{\varphi}|\sigma Y)+g(\tau|\boldsymbol{\varphi}|\sigma Y)g(\tau|\boldsymbol{\varphi}|\sigma Y'')\right]\\ &= 2\sigma\rho_4 E\left[Yg(\tau|\boldsymbol{\varphi}|\sigma Y)\right]+E\left[g(\tau|\boldsymbol{\varphi}|\sigma Y)g(\tau|\boldsymbol{\varphi}|\sigma Y'')\right],\end{aligned}$$

where X, Y, and Y'' are correlated standard normals with $\rho_4=\mathsf{Corr}(X,Y)=2/(3|\varphi|)$ and $\rho_5=\mathsf{Corr}(Y,Y'')=-14/(9|\varphi|^2)$.

Combining all of three computations, we arrive at

$$\begin{aligned}&E[(A_{i+1}-2A_i+A_{i-1})^2]\\ &= 6\sigma^2-\frac{70\sigma}{3|\varphi|}E\left[Yg(\tau|\boldsymbol{\varphi}|\sigma Y)\right]+6E\left[g(\tau|\boldsymbol{\varphi}|\sigma Y)^2\right]\\ &\quad + 2E\left[g(\tau|\boldsymbol{\varphi}|\sigma Y)g(\tau|\boldsymbol{\varphi}|\sigma Y')\right]\\ &\quad - 8E\left[g(\tau|\boldsymbol{\varphi}|\sigma Y)g(\tau|\boldsymbol{\varphi}|\sigma Y'')\right].\end{aligned}$$

The next step is to represent each of these terms in their simplest forms so that numerical implementation becomes straightforward. First of all,

$$\begin{aligned}&E\left[Yg(\tau|\boldsymbol{\varphi}|\sigma Y)\right]\\ &= E\left[\delta\sigma Y;\, Y>\frac{\delta}{\tau|\boldsymbol{\varphi}|}\right]-E\left[\delta\sigma Y;\, Y<-\frac{\delta}{\tau|\boldsymbol{\varphi}|}\right]\\ &\quad + E\left[\tau|\boldsymbol{\varphi}|\sigma Y^2;\,|Y|\le\frac{\delta}{\tau|\boldsymbol{\varphi}|}\right]\\ &= 2\delta\sigma E\left[Y;\,Y>\frac{\delta}{\tau|\boldsymbol{\varphi}|}\right]+\tau|\boldsymbol{\varphi}|\sigma E\left[Y^2;\,|Y|\le\frac{\delta}{\tau|\boldsymbol{\varphi}|}\right].\end{aligned}$$

where we used the symmetric property of Y. For notational convenience, we write x for $\delta/(\tau|\boldsymbol{\varphi}|)$. Then, secondly,

$$\begin{aligned}E[g(\tau|\boldsymbol{\varphi}|\sigma Y)^2] &= (\delta\sigma)^2P(|Y|>x)\\ &\quad +(\tau|\boldsymbol{\varphi}|\sigma)^2E[Y^2;\,|Y|\le x].\end{aligned}$$

For the third term, we have:

$$\begin{aligned}&E\left[g(\tau|\boldsymbol{\varphi}|\sigma Y)g(\tau|\boldsymbol{\varphi}|\sigma Y')\right]\\ &= 2(\delta\sigma)^2P(Y>x,\,Y'>x)-2(\delta\sigma)^2P(Y>x,\,Y'<-x)\\ &\quad +4\tau|\boldsymbol{\varphi}|\delta\sigma^2E\left[Y;\,|Y|\le x,\,Y'>x\right]\\ &\quad +(\tau|\boldsymbol{\varphi}|\sigma)^2E\left[YY';\,|Y|\le x,\,|Y'|\le x\right].\end{aligned}$$

Similar computations are made for the last term. We sum them up and divide it by $6\sigma^2$, obtaining the formula in the statement. ■

Biographies

Wanmo Kang is an Assistant Professor in the Department of Mathematical Sciences at KAIST. He received his Ph.D. in Operations Research from Columbia University. He is interested in applied probability and risk analytics.

Kyoung-Kuk Kim received his Ph.D. from Columbia Business School. He also has B.S. and M.S. degrees in Mathematics from Seoul National University and Stanford University, respectively. After spending a year in the finance industry, he has been in the Department of Industrial and Systems Engineering at KAIST since 2009. His research interests include stochastic processes, stochastic simulation, and risk management.

Hayong Shin is a Professor in the Department of Industrial Engineering at KAIST. He received a B.S. from Seoul National University and an M.S. and a Ph.D. from KAIST, all in Industrial Engineering. His current research interests are in the area of geometric modeling, computational geometry, and Monte Carlo simulation.